PROFILING THE INTERACTOME OF STK10

BY USING PROXIMITY-BASED BIOTINYLATION

A THESIS SUBMITTED TO

THE GRADUATE SCHOOL OF ENGINEERING AND SCIENCE

OF BILKENT UNIVERSITY

IN PARTIAL FULFILLMENT OF THE REQUIREMENTS FOR

THE DEGREE OF

MASTER OF SCIENCE

IN

MOLECULAR BIOLOGY AND GENETICS

By

Yağmur Öykü Carus

May 2023

PROFILING THE INTERACTOME OF STK10

BY USING PROXIMITY-BASED BIOTINYLATION

By Yağmur Öykü Carus

May 2023

We certify that we have read this thesis and that in our opinion it is fully adequate, in scope and quality, as a thesis for the degree of Master of Science.

Onur Çizmecioğlu (Advisor)

Mesut Muyan

Özlen Konu Karakayalı

Approved for the Graduate School of Engineering and Science:

Orhan Arıkan

Director of the Graduate School

ABSTRACT

PROFILING THE INTERACTOME OF STK10

BY USING PROXIMITY-BASED BIOTINYLATION

“Yağmur Öykü Carus”

M.S. in Molecular Biology and Genetics

Advisor: Onur Çizmecioğlu

May 2023

Breast cancer accounts for a quarter of all newly diagnosed cancer cases globally in women. It is also the primary cause of death in female cancer patients. In 2020, it was responsible for 15% of all cancer-related deaths in women. The PI3K pathway is the most commonly deregulated pathway in breast cancer. As a result, numerous inhibitors for druggable targets within the pathway have been developed. Unfortunately, drug resistance is frequently observed after treatment with these inhibitors. The mechanisms behind this resistance are widely studied. AKT has been known to be the kinase responsible for transmitting the signal to downstream targets. However, new studies suggested there can be AKT-independent kinases relaying the signal to downstream targets causing PI3K inhibitor drug resistance.

Previously, our group hypothesized that they could find an AKT-independent protein that confers resistance to PI3K inhibition. Their bioinformatical analyses identified STK10 (Serine-Threonine Kinase 10) as a possible druggable target for PI3K pathway inhibitor resistance in an AKT-independent manner. They performed wet lab experiments to show STK10’s impact on PI3K inhibitor resistance in breast cancer. They showed STK10 knock-down sensitizing resistant breast cancer cells to PI3K

inhibitor. Although their experiments supported the hypothesis of STK10 affecting the PI3K inhibitor resistance of breast cancer cells, they could not identify the molecular mechanisms behind this interaction.

In this study, by using APEX2 proximity-based biotinylation followed by mass spectrometry, we profiled STK10's interactome. We aimed to understand how STK10 contributes to the progression of breast cancer and the development of resistance to treatment. Our bioinformatics analyses indicated possible interaction between STK10 and the candidate proteins we obtained from our mass spectrometry analysis. Immunofluorescence and Co-IP experiments supported some of the putative interactions we discovered. The proteins discovered near STK10 were primarily linked to the reorganization of the cytoskeleton, which is encouraging since STK10 is recognized for its involvement in cell migration through the phosphorylation of ERM proteins. Based on our observations, it is possible to hypothesize that STK10 is influencing the cytoskeletal reorganization in breast cancer cells. However, further experiments are needed to be done to understand the molecular mechanisms behind STK10's possible functions in breast cancer. These experiments could lead to uncovering the role of STK10 in PI3K inhibitor resistance and help us to identify new therapeutic options to battle breast cancer.

Keywords: Breast cancer, STK10, proximity biotinylation, APEX2, proteomics, mass spectrometry, cytoskeletal proteins.

ÖZET

STK10 ile ETKİLEŞEN PROTEİNLERİN PROKSİMİTE TEMELLİ BİYOTİNLEME İLE PROFİLLENMESİ

“Yağmur Öykü Carus”

Moleküler Biyoloji ve Genetik, Yüksek Lisans

Tez Danışmanı: Onur Çizmecioğlu

Mayıs 2023

Meme kanseri, dünya çapında kadınlarda yeni teşhis edilen tüm kanser vakalarının dörtte birini oluşturmaktadır. Aynı zamanda kadın kanser hastalarında birincil ölüm nedenidir. 2020 yılında kadınlarda kansere bağlı tüm ölümlerin %15'ini meme kanserine bağlı ölümler oluşturdu. meme kanserinde en sık değişkenliğe uğrayan yolağı PI3K yolağıdır. Bundan dolayı, PI3K yolağı içindeki hedeflenebilir proteinler için çok sayıda inhibitör geliştirilmiştir. Ne yazık ki, bu inhibitörlerle yapılan tedaviler sonrası hastalarda ilaç direnci sıklıkla gözlenmektedir. Bu direncin arkasındaki mekanizmalar araştırma grupları tarafından sıklıkla çalışılıyor. PI3K sinyalini iletmekten sorumlu en önemli kinazın AKT olduğu düşünülse de, yeni araştırmalar, bu sinyali PI3K yolağının altında bulunan proteinlere ileten AKT'den bağımsız kinazlar olabileceğini, ayrıca, bu tip kinazların PI3K inhibitörü ilaç direncine neden olabileceklerini öne sürdü.

Buna dayanarak, grubumuz daha önceki çalışmalarında, PI3K inhibisyonuna direnç sağlayan AKT'den bağımsız benzeri bir kinaz bulabileceklerini varsaymıştı. Biyoinformatik analizleri, STK10'u (Serin-Treonin Kinaz 10) AKT'den bağımsız bir şekilde PI3K yolağı inhibitörü direnci için olası bir hedeflenebilir bir protein olarak

tanımladı. STK10'un meme kanserinde PI3K inhibitörü direnci üzerindeki etkisini göstermek için laboratuvar deneyleri gerçekleştirdiler. Bu deneyler sonucunda STK10'un, dirençli meme kanseri hücrelerini PI3K inhibitörüne karşı hassaslaştırdığını gösterdiler. Deneyleri, STK10'un meme kanseri hücrelerinde PI3K inhibitör direncini etkilemesi hipotezini desteklese de, bu etkileşimin arkasındaki moleküler mekanizmaları tanımlayamadılar.

Bu çalışmada, APEX2 proksimite temelli biyotinleme ve ardından kütle spektrometrisi kullanarak, STK10'un interaktomunun profilini çıkardık. STK10'un meme kanserinin ilerlemesine ve tedaviye direnç gelişimine nasıl katkıda bulunduğunu öğrenmeyi amaçladık. Biyoinformatik analizlerimiz, ve kütle spektrometresi analizimizden elde ettiğimiz aday proteinler ve STK10 arasındaki olası bir etkileşimi gösterdi. İmmünofloresan ve Co-IP deneylerimiz de bu olası etkileşimleri destekledi. Deneylerimiz sonrası tespit ettiğimiz STK10'un yakınında bulunan proteinler, öncelikle hücre iskeletinin yeniden düzenlenmesi ile bağlantılı proteinlerdi. Bu, STK10'un, ERM proteinlerinin fosforile ederek hücre göçüne katılımıyla tanınması nedeniyle cesaret vericidir. Gözlemlerimize dayanarak, STK10'un meme kanseri hücrelerinde hücre iskeletinin yeniden yapılanmasını etkilediğini varsaymak mümkün. Ancak, STK10'un meme kanserindeki olası işlevlerinin ardındaki moleküler mekanizmaları anlamak için daha fazla deney sonucuna ihtiyacımız var. Yapılacak bu deneyler, STK10'un PI3K inhibitör direncindeki rolünün ortaya çıkarılmasına yol açabilir ve meme kanseriyle savaşmak için yeni terapötik seçenekler belirlememize yardımcı olabilir.

Anahtar Kelimeler: Meme kanseri, STK10, yakınlık tabanlı biyotinleme, APEX2, proteomik, kütle spektrometrisi, hücre iskeleti proteinleri.

ACKNOWLEDGEMENTS

I would like to express my sincere gratitude to my thesis advisor Asst. Prof. Onur Çizmecioğlu, for giving me the opportunity to work under his guidance and for his invaluable support throughout my master's. His knowledge, insights, and feedback helped me so much. I feel very lucky to have been his student.

I want to thank all of the OC lab members for their friendships and academic help. The supportive and friendly people of this lab showed me how important it is to have a healthy work environment. They are amazing people with bright minds. I hope I will have the luck to work with people like them in my future academic career. I also want to thank our third-floor group. Working alongside them was great, I have so many happy memories with them. I also want to thank my first intern Melike Ergüven for being a great student. I discovered how much I enjoyed teaching during my year as her teaching assistant.

I would like to extend a special thanks to my previous teachers and supervisors, Dr. Mari Kaarbo and Asst. Prof. Nihal Terzi Çizmecioğlu. Their guidance helped me throughout my academic life. I also want to thank Prof. Işık Yuluğ and Prof. Chang-Duk Jun for helping us by providing the products we needed to perform crucial experiments.

I want to especially thank my amazing best friends Beril Daloğlu, Mahnoor Sulaiman and Sera Zenginler. They are one of the best things that Bilkent has given me. Their love, kindness, and support helped me get through the hardest times. I cannot emphasize enough how valuable they are to me.

I also want to thank my friends Dersu Sezginmert, Esra Başaran and Aykut Alagöz. Their friendships throughout these years were really valuable to me.

I want to thank my parents, Zehra and Ramazan Carus. Whatever accomplishment I have is thanks to their unconditional love and support. I want to thank my sister Burcu Mutlu for her love, patience, and help. Together with my brother-in-law Erdal Mutlu, they always guided me whenever I needed. I want to thank my little nephew Rüzgar Ege Mutlu for being a constant source of joy in my life. I want to thank Selim Şahin for making my life brighter. With his limitless love and patience, everything became easier. He has been my support system and my source of motivation.

I would like to also thank TUBITAK for granting me Bideb 2210A National M.Sc. Scholarship and funding this project (Project no: 1002-120Z832).

Table of Contents

LIST OF FIGURES

LIST OF TABLES

ABBREVIATIONS

PI3K	Phosphatidylinositol-3 kinase
PTEN	Phosphatase and tensin homolog
TNBC	Triple negative breast cancer
PIP3	Phosphatidylinositol-3,4,5-triphosphate
PIP2	Phosphatidylinositol-4,5-bisphosphate
AKT	Serine/threonine kinase
mTOR	Mammalian target of rapamycin
HER2	Human epidermal growth factor receptor 2
PR	Progesterone receptor
ER	Estrogen receptor
GFP	Green fluorescent protein
RFP	Red fluorescent protein
APEX2	Ascorbate peroxidase 2
RTK	Receptor Tyrosine Kinase
GPCR	G-Protein coupled receptor
IP	Immunoprecipitation
HMEC	Human Mammary Epithelial Cells

1. INTRODUCTION

1.1. Breast Cancer

Worldwide, 2,3 million women were diagnosed with breast cancer in 2020, and 685 thousand women lost their lives to this disease. In the majority of the world, breast cancer has the highest incidence rate in females, accounting for one in four new cases **(Figure 1.1.)** [1]. Breast cancer is also the top cancer type causing the deaths of female patients. Approximately 15% of the women who lost their lives to cancer died because of breast cancer in 2020 **(Figure 1.2.)**. The incidence of breast cancer increases with age, and it affects women of all ages globally after puberty[2]. In 2023, it is expected that 609,820 Americans will have lost their lives to cancer, which corresponds to an average of 1670 people per day. In females, the most common causes of death due to cancer are expected to be those of the breast, lung, and colorectum [3].

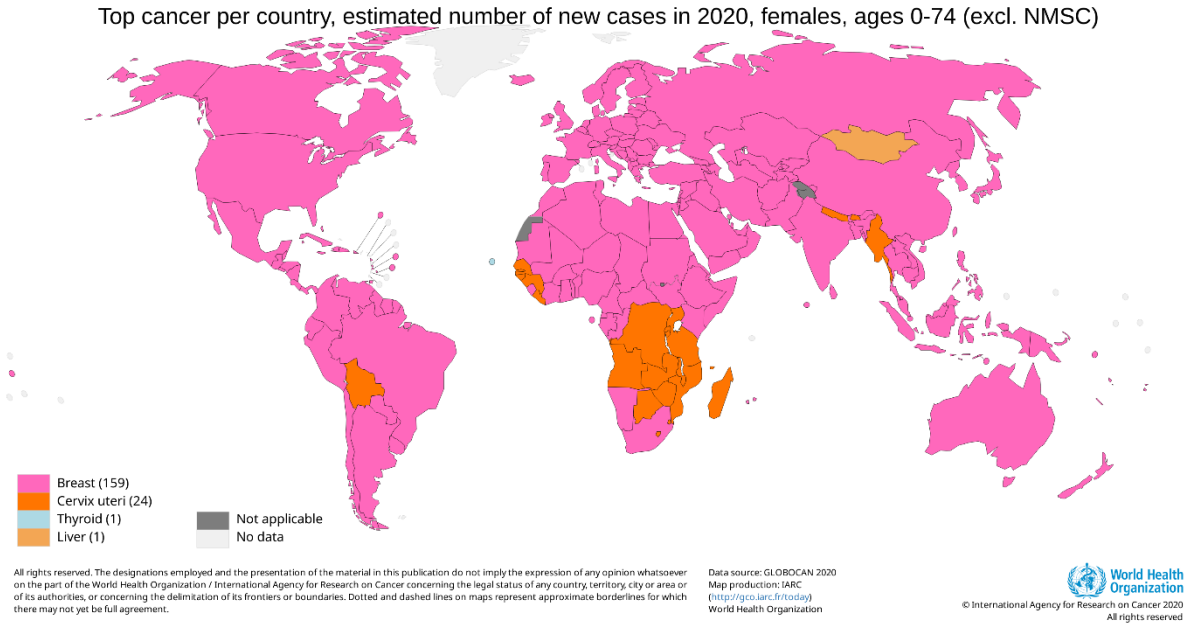

Figure 1. 1 The estimated incidence rate of cancer in the world in 2020. An illustration showing the estimated number of new cancer cases in 2020 for females according to the most common sites of cancer incidence. Pink indicates breast cancer [1].

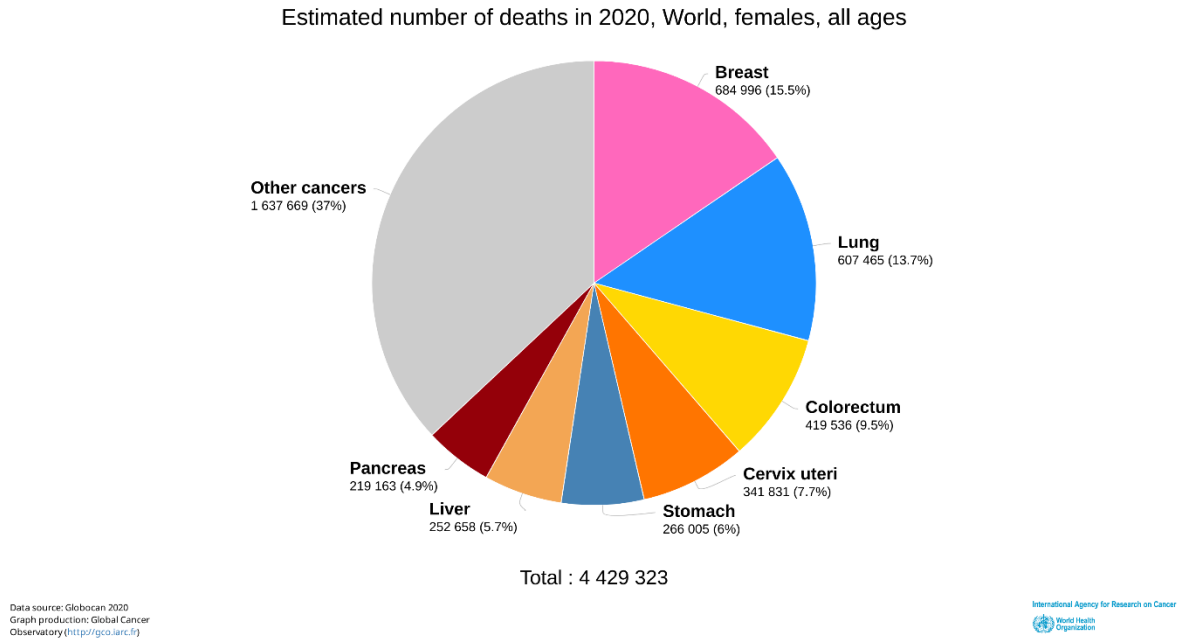

Figure 1. 2 Estimated number of cancer deaths worldwide for females. A pie chart showing the estimated mortality of female cancer patients according to their cancer types in 2020.(Cancer Today, 2020)

Early breast cancer that has not spread from the breast tissue or has only spread to the axillary lymph nodes is considered highly treatable, whereas metastatic breast cancer is not curable with the current treatments[4]. There are several subtypes of breast cancer that were classified by the differences in their molecular characteristics. In 2000, Perou and Sorlie reported four distinguished subtypes of breast cancer: Luminal A (ER+,HER2-), luminal B(ER+), basal-like (ER-,PR-,HER2-), and human

epidermal growth factor receptor 2 (HER2) enriched(HER2+) [5]. Other than this classification, in clinics, a surrogate classification of breast cancer is also used. In this classification, there are five subtypes: hormone receptor-positive breast cancers; HER2 enriched, luminal B like HER2+, luminal B like HER2-, luminal A like and hormone receptor-negative breast cancer called triple-negative breast cancer(TNBC)[4]. TNBC subtype does not express progesterone receptor (PR), estrogen receptor (ER), or human epidermal growth factor receptor 2 (HER2). It has a poor prognosis, high metastasis chance, and a high risk of invasiveness. Furthermore, it is harder to treat compared to the other subtypes of breast cancer because of its lack of PR, ER, and HER2, which are the main target of current treatments for breast cancer. New treatment options need to be developed for TNBC since there is still no treatment standardized for it [6].

1.2. PI3K/AKT Pathway

The phosphoinositide-3-kinase (PI3K) pathway is the most frequently activated pathway in human cancers. Its deregulation causes tumorigenesis because it plays a crucial role in the proliferation, growth, metabolism, and survival of cells **(Figure 1.3)**. Phosphoinositide 3-kinase (PI3K) is a lipid kinase found in membranes and has two subunits, p85 and p110. The PI3K regulatory subunit, p85, and the catalytic subunit, p110[7]. The regulatory subunit p85 stabilizes the catalytic subunit p110 and inhibits it in the inactive state of the pathway. p110 has different isoforms; p110α, p110β, and p110δ. They are encoded by PIK3CA, PIK3CB, and PIK3CD genes, respectively. The expression of p110 isoforms p110α and p110β is found in nearly all tissues, whereas p110δ expression is mostly seen in the immune system. The N-terminal p85-binding domain, the RAS-binding domain, the C2 membrane-binding domain, the helical domain, and the C-terminal catalytic domain are the five common domains shared by

all p110 isoforms. There are also 5 distinct isoforms of the p85 regulatory subunit: p85α, its splice variants p55α and p50α, p85β and p55γ[8]. Inter-Src Homology domain (iSH2) and two SH2 domains are common in these p85 isoforms. The iSH2 domain functions as the binding point of p85 to p110.

PI3K has three different classes which are I,II, and III. Class IA PI3K can be activated by receptor tyrosine kinases, G protein-coupled receptors (GPCR), and some small GTPases. PDGF receptor (PDGFR), epidermal growth factor receptor (EGFR), insulin-like growth factor receptor (IGFR), and insulin receptor (INSR) are some of the well-known growth factor receptors that activate Class IA PI3K. Different from Class IA PI3K, Class IB PI3K is activated only by GPCRs. Of the PI3K classes, Class IA PI3K is the one that has been studied the most.

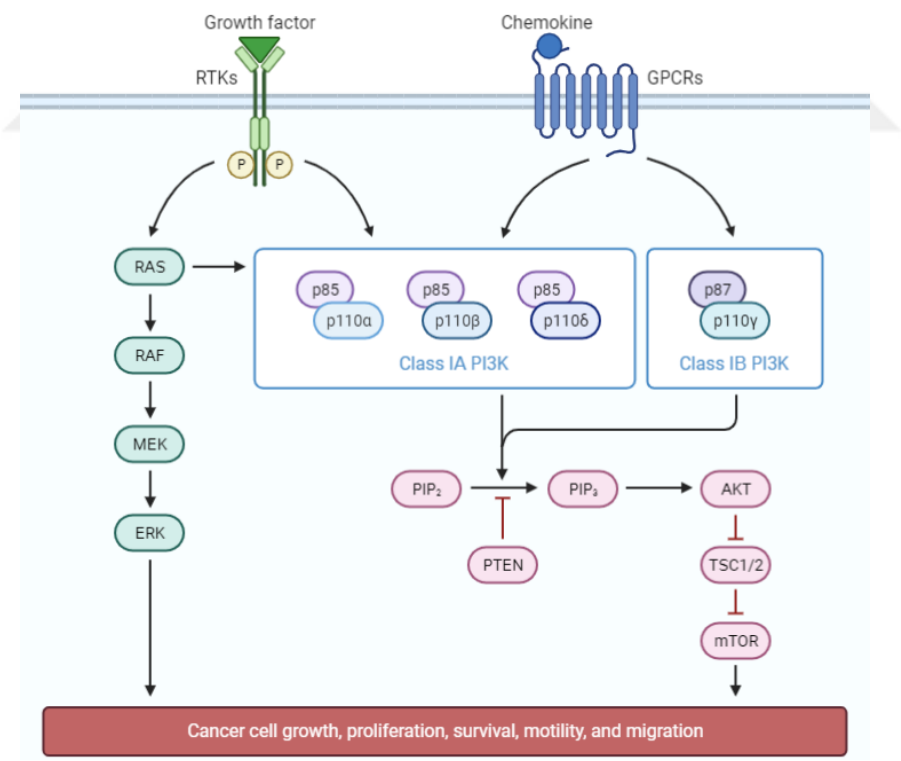

Figure 1. 3 Schematic representation of PI3K Pathway.

Created by Biorender.**[9]**

Upon ligand binding to RTKs, the receptor's tyrosine residues get phosphorylated. These phosphorylated residues interact with regulatory subunits of Class IA PI3K and lead to the recruitment of p110 to the plasma membrane. p110 is then activated at the plasma membrane and this activation triggers its catalytic function which is converting phosphatidylinositol (3,4)-biphosphate (PIP2) to phosphatidylinositol (3,4,5)-triphosphate (PIP3). With the production of PIP3, 3-phosphoinositide-dependent kinase 1 (PDK1) and AKT are recruited to the plasma membrane. Here, AKT gets phosphorylated at its Threonine 308 residue and gets partially activated. AKT also gets phosphorylated by the mammalian target of rapamycin complex 2 mTORC2 at its Serine 273 residue. This leads AKT to get fully activated and trigger the phosphorylation of the downstream signaling targets. These downstream targets include PRAS40 and TSC2. Phosphorylation of these two targets causes their inhibitory effects on mTORC1 to cease. The activated mTORC1 phosphorylates its targets, including 4EBP1 and ribosomal protein S6, to promote cell proliferation[7].

1.3. Breast Cancer Treatments and PI3K Pathway

PI3K/AKT/mTOR pathway is a frequently activated pathway in breast cancer. Furthermore, in ER+ breast cancer, PIK3CA, which encodes the p110a isoform, is the most commonly mutated gene. Human epidermal growth factor receptor 2 (HER2)-directed therapy, cytotoxic therapy, and endocrine therapy have all been associated with decreased response rates in breast cancer patients who have the PI3K pathway activated [10]. The inhibitors used for the treatment of breast cancer include mTOR inhibitors for HER2 negative HR-positive breast cancer, PI3K, AKT and mTORC inhibitors. However, these inhibitors have a distinct spectrum of side effects that call for specialized care and treatment techniques [10].

1.4. STK10 Kinase

STK10(Serine Threonine Kinase 10) also called lymphocyte-oriented kinase (LOK) is a member of Ste20 family kinases. It has an N terminak kinase domain and C terminal coiled coil domain. STK10 has similar qualities as polo-like kinase kinases. It has been known to phosphorylate PLK1. Its kinase-dead version had been suggested to cause abnormal cell cycle progression. Furthermore, it has some negative effects on IL2 expression in T-Cells [11]. STK10 is also involved in the lymphocyte migration process via its phosphorylation activity on ERM (Ezrin-Radixin-Moesin) proteins like MSN [12]. Ezrin, radixin, and moesin are all members of the ERM protein family, and they work together to control cell shape, adhesion, migration, and division by connecting actin filaments to the plasma membrane. Furthermore, STK10 negatively regulates MAP3K1/MEKK1[13].

In the literature, there is no study that identified STK10's function on breast cancer. However, it has been associated with some other cancer types. In a study, wild-type STK10 was found to be a suppressor of NFkB activity and a potentiator of dexamethasone-induced apoptosis in Peripheral T-cell lymphoma (PTCL) cells. High throughput resequencing of these cells revealed a missense mutation (c.2201G>A) in STK10 cDNA replacing arginine residue with histidine (R634H). This change in the sequence has abolished NFkB suppression caused by STK10 and led to a significant decrease in the pro-apoptotic activity of the cells. So, it can be said that STK10 might act like a tumor suppressor in PTCL cells[14]. In another study, scientists tested several Ewing's sarcoma cell lines in high throughput-RNAi screens by knocking down 572 kinases with the use of a siRNA library. In this study, STK10 knock-down caused a reduction in the proliferation rate of Ewing's sarcoma cells. Furthermore, this knock-down led to increased apoptosis in these cells [15]. Another group worked on STK10's

possible role in tumor migration and invasion. In their first study, these researchers showed that the knockout of STK10 causes migration and invasion in cervical cancer[16]. Also, the same group investigated the effect of STK10 KO on prostate cancer, and their experiments indicated that STK10 might promote cell growth and prevent cell death by suppressing p38 MAPK in prostate cancer cells [17]. STK10 is also associated with lymphoid cancers, which is anticipated by looking at the expression levels of STK10 throughout the body. It is mostly expressed in lymphoid tissues. STK10 is also a prognostic marker of colorectal cancer, according to Human Protein Atlas[18].

Although some of these findings about STK10 contradict, they suggest that STK10 has some role in tumor progression, which varies between different tumor types. Since its effect on breast cancer has not been investigated before our group, exploring these effects is crucial for understanding the molecular mechanisms behind breast cancer and STK10's possible involvement with them.

1.5. STK10 as a target for PI3K pathway inhibitor resistance

Recent studies have linked well-characterized kinases with resistance to PI3K inhibition through AKT-independent mechanisms[19], [20]. However, since AKT has been singled out as the primary node through which the PI3K pathway mediates tumorigenesis, the roles of such kinases in cancer have been largely ignored. To overcome PI3K inhibitor resistance in breast cancer, new therapeutic approaches can be developed. For this purpose, new molecular targets should be identified.

Previously, our group hypothesized that we could find a protein working in an AKT-independent way that confer resistance to PI3K inhibition[21]. To find these possible proteins, in their previous study, our group did bioinformatical analyses using online

cancer databases and identified STK10 as a possible druggable target for PI3K pathway inhibitor resistance in an AKT-independent way **(Figure 1.4.)**. They measured 70 of 84 breast cancer cell lines were for mRNA expression sensitivity to 138 compounds. They found 196 upregulated genes in PIK3CA-mutated breast cancer cell lines that were resistant to PI3K/AKT/mTOR inhibition. They eliminated 150 genes positively correlated with AKT phosphorylation using TCGA RPPA data. Then, they found 12 genes that predict survival in PIK3CA mutation patients using the METABRIC dataset. Finally, they used published mRNA expression data from MCF10A cells expressing ectopic mutant PI3K (H1047R) to identify STK10 as a gene with significantly higher expression levels than control cells.

After this identification, they performed wet lab experiments, including siRNA knockdown of STK10, growth assays, and STK10 overexpression assays. Their results showed elevation of STK10 in PI3K pathway inhibitor-resistant luminal A T47D cells; also, they showed siRNA knock-down of STK10 re-sensitizing the PI3K inhibitor-resistant cells.

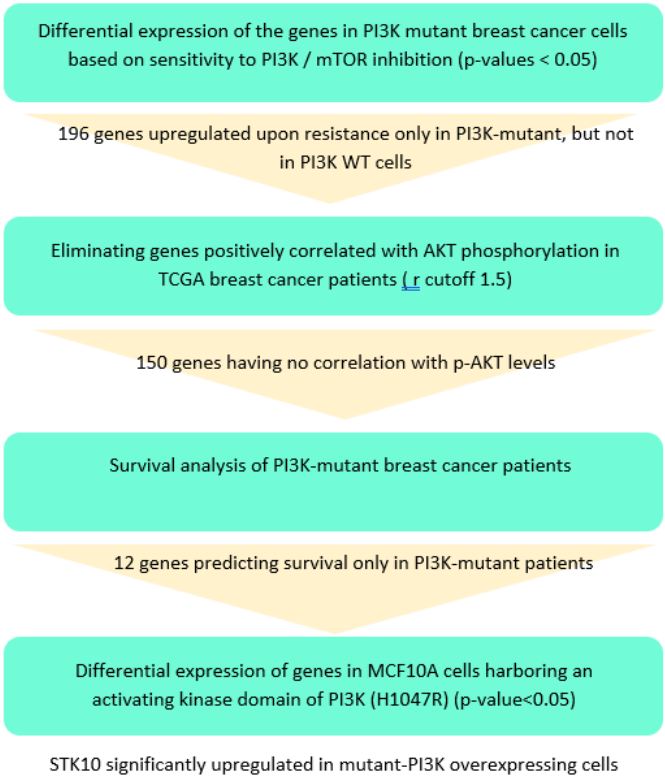

Figure 1. 4 Identification of STK10 as a potential target for inhibitor resistance of the PI3K pathway that is independent of AKT. Workflow of the bioinformatical analyses performed in order to identify STK10 as having a possible role in the inhibitor resistance of the PI3K/AKT pathway in an AKT independent way(Tarman, 2020).

All these indicated a possible interaction between the PI3K pathway and STK10, leading to PI3K inhibitor resistance. However, they could not identify how STK10 is working toward this inhibitor resistance mechanistically[21].

1.6. Protein-Protein Interaction Analysis Methods

Protein-protein interactions are crucial for a lot of biological processes important for the health of cells. To understand these processes and their dysregulations, an analysis of protein-protein interactions is needed. Some traditional methods for protein-protein interaction analysis are co-immunoprecipitation, affinity purification and yeast two-hybrid system. In combination with mass spectrometry-based proteomics, antibody-based affinity purification enables the identification of stable interaction partners of proteins of interest[22]. Yeast two-hybrid system allows researchers to screen thousands of molecular interactions. Although these methods were widely used, they have some limitations. For instance, with affinity purification, weak or transient interactions may be lost while performing the lysis or wash steps. With yeast two hybrid system, there may be cell type restrictions. With immunoprecipitation, only the stable interacting partners can be captured, the weak or transient interactions may be lost during the washing steps[23].

1.7. Proximity-based biotinylation

To overcome the limitations of the other protein-protein interaction methods, new methods were developed. Proximity labeling was one of these developed methods. It is a technique for tagging the endogenous interaction partners of specific proteins through genetic fusion to enzymes that catalyze the formation of diffusible reactive species in living cells. After that, tagged molecules that interact with the protein of interest can be purified and identified using mass spectrometry or nucleic acid sequencing [22]. Proximity labeling-based methods combined with mass spectrometry (MS) provide a high-throughput method for analyzing spatially restricted proteomes. Furthermore, these methods are useful for understanding cellular organization and protein interactome networks within the cells.

In more detail, proximity labeling makes use of some engineered enzymes, including engineered ascorbate peroxidase 2 (APEX2), horse radish peroxidase (HRP), biotin ligases (BioID, BASU, TurboID) that generate reactive radicals. These radicals can covalently bind to nearby proteins. Both the half-life of the reactive species and the concentration of quenchers in the environment influence the labeling radius[22]. The tagged proteins can then be isolated and analyzed further using mass spectrometry. To analyze protein-protein interactions, the enzyme is fused to specific proteins or signal peptides targeting specific subcellular regions. This way, spatial expression is achieved, and it is ensured that only the proteins in the proximity of the fusion protein are tagged. By tagging regional proteomes, proximity labeling avoids the issues associated with conventional organelle purification methods and enables proteomic analysis of other types of subcellular regions[24]. In addition to this, since proximity labeling can be done in living cells, the protein-protein interactions can be studied in physiologically relevant conditions.

Although proximity labeling-based methods are helpful for characterizing protein interactome networks, they also have some disadvantages. One of these disadvantages is that it is not possible to differentiate the direct binding of two proteins from proteins being just adjacent to each other. Because of this, it is necessary to perform extensive follow-up studies in order to verify the results of proximity labeling experiments.

1.8. APEX2 enzyme

There are several different proximity labeling enzymes, each of them having its unique features. APEX2 is one of these enzymes. Ascorbate peroxidase (APEX) has recently been produced by Ting et al. to define the molecular environment surrounding a target protein by generating free reactive radicals of biotin-tyramide when hydrogen peroxide is given to the cells. This technique is known as “peroxidase-catalyzed proximity labeling” [23].

Most modern proximity labeling research employs an improved version of APEX (called APEX2) that has greater labeling efficiency. It is small protein with a size of 27 kDa. In the presence of H_2O_2, APEX2 catalyzes the oxidation of biotin-phenol (biotinyl tyramide) to the short-lived biotin phenoxyl radical **(Figure 1.5.)**. This radical reacts with electron-rich amino acids like tyrosine on neighboring proteins within the radius of several nanometers. This results in the biotinylation of the proteins in the proximity of APEX2. A construct producing the protein of interest fused with APEX2 enzyme can be used in order to label the interactome of the protein of interest **(Figure 1.5)**.

There are some advantages of using APEX2. For instance, labeling with APEX2 enzyme is fast compared to BioID. The labeling takes around 1-2 minutes with APEX2,

whereas it takes hours with BioID. Since APEX2 works really fast, the non-specific biotinylation rate is lower than the other biotinylation enzymes. Also, thanks to its small

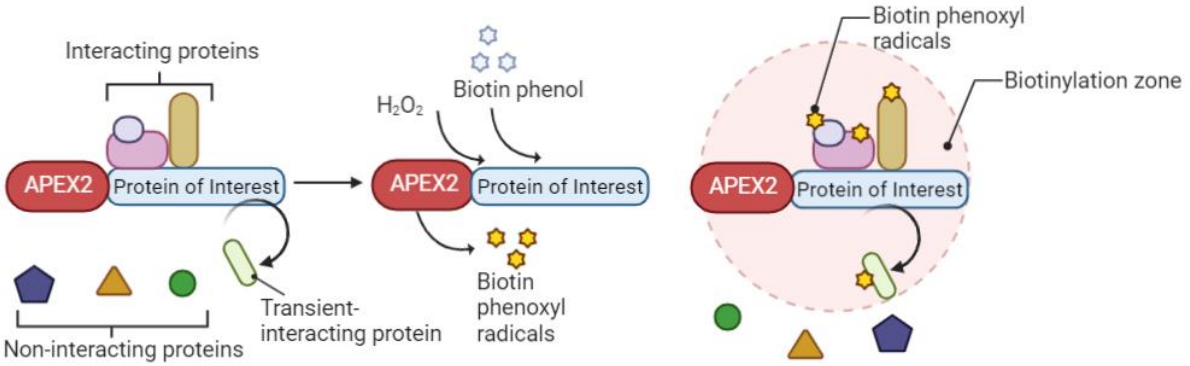

Figure 1. 5 The working principle of APEX2 enzyme. Created by Biorender.(BioRender, 2020).

size, it is less likely for APEX2 to interact sterically with the protein to which it is added. Additionally, with APEX2 proximity biotinylation, one can biotinylate not only the stable interaction partners but also the transient ones. One disadvantage of APEX2 is that it is not suitable for organoid or in vivo studies because of the toxicity of biotin phenol on living cells.

1.9. Rationale and aims of the study

Although our group's previous work suggested that STK10 may play a role in the PI3K pathway, which could cause resistance to PI3K inhibitors, they did not know how STK10 impacts the PI3K pathway. To understand the underlying mechanisms, in this project, we sought to define the interactome of STK10 utilizing proximity-based biotinylation. By doing this, we wanted to unravel a possible association of STK10 with the PI3K pathway and perhaps find a novel druggable target for breast cancers resistant to PI3K pathway inhibitors.

2. MATERIALS AND METHODS

2.1 Materials

2.1.1. Cell Culture Media and Supplements

Catalog Number	Product Name	Brand
41966-029	High Glucose DMEM	Gibco, US
11-320-033	DMEM / F-12	Gibco, US
25300-054	Trypsin-EDTA (0.05%)	Gibco,US
S1810-500	Fetal Bovine Serum (FBS)	Biowest, US
15140-122	Penicillin-Streptomycin	Gibco,US
P04-80100	L-Glutamine	PAN Biotech, Germany
1H72652	PBS, 10X pH 7.4	BioShop, Canada
AF-100-15	Epidermal growth factor (EGF)	Peprotech, London, UK
50-23-7	Hydrocortisone	Sigma Aldrich, USA
I9278	Insulin	Sigma Aldrich, USA
Sc-134220	Polybrene	Santa-Cruz Biotech, USA
5100-0001	Mr. Frosty Freezing Container	Thermo Scientific, US
A111138-03	Puromycin	Gibco, US

2.1.2. Routinely Used Solutions

Solution	Ingredients
RIPA Cell Lysis Buffer	1X RIPA 1 µM DTT 1 mM Na3VO4 1X Phosphatase inhibitor mix 1X Protease inhibitor
NP-40 Lysis buffer	0.5% w/v NP-40 50mM Tris-HCl pH 7.5 150mM NaCl 5mM EDTA 1x. Protease Inhibitor 1x Phosphatase Inhibitor Mix 1mM DTT 0.1mM Na_3VO_4
Resolving Gel Buffer (pH=8.8)	187 g Trizma-Base pH adjustment with HCl Complete volume up to 1L with ddH2O
Stacking Gel Buffer (pH=6.8)	60.5 g Trizma-Base pH adjustment with HCl Complete volume up to 1L with ddH2O
10X Tris Buffered Saline (TBS)	80 g NaCl

	2 g KCl 30 g Trizma-Base pH adjustment to 7.4 with HCl Complete volume up to 1L with ddH2O
1X TBS-T	1L 1X Tris Buffered Saline 1mL Tween-20
10X SDS-PAGE Running Buffer	30 g Trizma-Base 144 g Glycine 10 g SDS Complete volume up to 1L with ddH2O
10X Western Blot Transfer Buffer	30 g Trizma-Base 144 g Glycine Complete volume up to 1L with ddH2O
Blocking Solution for Western Blot	5 mg Milk Powder or BSA 100 mL TBS-T
50X Tris Acetate Edta (TAE)	242 g Trizma-base 57.1 mL acetic acid 100 mL 0.5M EDTA Complete volume up to 1L with ddH2O
4% PFA Solution	4g Paraformaldehyde 100 mL PBS

2.1.3. Chemicals

Catalog Number	Product Name	Brand
SE3017501	Sodium Azide	Serva, Germany
238813	Trolox ((±)-6-Hydroxy-2,5,7,8-tetramethylchromane-2-carboxylic acid)	Sigma Aldrich, USA
E301-100G	Sodium Ascorbate	Smart Kimya, Turkey
106392	Sodium Carbonate (Na2CO3)	Merck, Germany
51456-500G	Urea	Sigma Aldrich, USA
22582	Biotin	Cayman Chemical, USA
41994-02-9	Biotinyl Tyramide (Biotin Phenol)	Cayman Chamical,USA
31434-1KG- R	Sodium chloride	Sigma Aldrich, USA
T1503-1KG	Trizma Base	Sigma Aldrich, USA
E0301-100	Agarose	EurX, Poland
1.08421	EDTA	Merck, Germany
E-7637	Ethidium Bromide	Sigma Aldrich, USA
7447-40-7	Potassium Chloride (KCl)	Merck, Germany
C3306	Calcium Chloride Dihydrate	Sigma Aldrich, USA
1058331000	Magnesium Chloride Hexahydrate	Merck, Germany
216763	Hydrogen Peroxide Solution	Sigma Aldrich, USA

2.1.4. Cloning Related Products

Catalog Number	Product Name	Brand
R3136S	BamHI-HF Restriction Enzyme	NEB,USA
R3101S	EcoRI-HF Restriction Enzyme	NEB,USA
R3138S	SalI-HF Restriction Enzyme	NEB,USA
M0202S	T4 DNA Ligase	NEB,USA

M0371S	Shrimp Alkaline Phosphatase	NEB,USA
N3232S	NEB 1kB DNA Ladder	NEB,USA
C3040I	Competent E.coli Cells	NEB,USA
48501.01	LB Mix	Serva, Germany
M0491S	Q5 DNA Polymerase	NEB,USA
	10-beta-Stable Outgrowth	
B9035	Medium	NEB,USA
05039-500G	Agar	Sigma Aldrich, USA

2.1.5. Reagents / Consumables

Catalog Number	Product Name	Brand
773301	Prime-Step Protein Ladder	BioLegend, US
161-0747	Laemmli Sample Buffer (4x)	Bio-Rad, US
34580	SuperSignal™ West Chemiluminescent Substrate	Sigma Aldrich, USA
10688.01	Acrylamide/Bisacrylamide Solution	Serva, Germany
11930.03	Albumin Bovine Fraction V, pH 7.0	Serva, Germany
927.033	Glycine	Isolab, Germany
39055.01	Phosphatase Inhibitor Mix	Serva, Germany
PIC002.1	Protease Inhibitor Cocktail	BioShop, Canada
P0758S	Sodium Orthovanadate	New England Biolabs, US

WHA10426892	Whatman Paper	Sigma Aldrich, USA
1215471	Nitrocellulose Membrane	GVS, China
2502	ReBlot Plus Mild Stripping Solution	Merck, Germany
M3148- 250ML	2- Betamercaptoethanol	Sigma Aldrich, USA
A40000279	Ponceau S Staining Solution	Thermo Scientific, US
23238	Pierce™ Coomassie Plus (Bradford) Assay Reagent	Thermo Scientific, US
458.22050.100	SDS	
960.151	Tween 20	Isolab, Germany
1.107.320.100	TEMED	Merck, Germany
24137-2.5L-R	Isopropapanol	Sigma Aldrich, USA
24229-2.5L-R	Methanol	Sigma Aldrich, USA
Sc-2003	Protein A/G PLUS-Agarose	Santa Cruz Biotechnology
3419S	Streptavidin Sepharose Beads	Cell Signaling Tech, USA

2.1.6. Antibodies

Catalog Number	Product Name	Brand
ab70484	Anti-LOK antibody	Abcam, UK
#3726	Phospho-Ezrin (Thr567)/Radixin (Thr564)/Moesin (Thr558)	Cell Signaling Technology ,USA

sc-47724	Anti-GAPDH Antibody	Santa Cruz Biotechnology, USA
405210	HRP Streptavidin	Biolegend, USA
SLBX2256	Monoclonal ANTI-FLAG® M2 antibody	Sigma Aldrich,USA
sc-9996	Anti-GFP (b-2)	Santa Cruz Biotechnology, USA
T0033	A tubulin - T003	Affiinity Biosciences
7076S	Anti-Mouse IgG, HRP-linked	Cell Signaling Technology, USA
7074S	Anti-Rabbit IgG, HRP-linked	Cell Signaling Technology, USA
405326	Alexa Fluor® 594 Goat anti-mouse IgG	Biolegend, USA

2.1.7. Proximity Biotinylation Experiment Stocks and Buffers

Chemical Stock Solutions

Reagent	Final Concentration	Storage
100X Trolox	500 mM (in DMSO)	Freshly prepared
100X Sodium ascorbate	1M (in sterile water)	Freshly prepared, kept on ice
100X Sodium Azide	1M (in sterile water)	Can be stored at 4 ^{o}C
Biotin Solution	50mM (in DMSO)	Can be stored at 4 ^{o}C

PBS^{++}

Ingredient	Final Concentration	Volume
10X PBS, pH 6.9	1X	5 mL
50mM $MgCl_2$	0.5mM	500 µL
100 mM $CaCl_2$	1mM	500 µL
Sterile ddH_2O		44 mL

Lysis Buffer

Ingredient	Final Concentration	Volume
RIPA Buffer		1.86 mL
25X Protease Inhibitor Coctail	1X	80 µL
100X Trolox	5 mM	20 µL
100X Sodium Ascorbate	10mM	20 µL
100X Sodium Azide	10mM	20 µL

Quenching Buffer

Ingredient	Final Concentration	Volume
10X PBS, pH 6.9	1X	5 mL
50mM $MgCl_2$	0.5mM	500 µL
100 mM $CaCl_2$	1mM	500 µL
100X Trolox	5mM	500 µL
100X Sodium ascorbate	10mM	500 µL
100X Sodium Azide	10mM	500 µL
Sterile ddH_2O		22.5 mL

Pull-Down Wash Buffers	Concentration
KCl	1M
Na_2CO_3	0.1 M
Urea in 10 mM Tris-HCl (pH8)	2M

Elution Buffer (1mL)

Ingredient	Final Concentration	Volume
4X Laemmli Buffer	2X	500 µL
1M DTT	200mM	200 µL
50mM Biotin Solution	15mM	300 µL

2.1.8. Kits

Catalog Number	Product Name	Brand
K0502	GeneJET Plasmid Mini Prep Kit	Thermo Scientific, US
12143	QIAGEN Midi Prep Kit (25)	Qiagen, Germany
K0691	GeneJET Gel Extraction Kit	Thermo Scientific, US
D6492-01	E.Z.N.A.® Cycle Pure Kit	OMEGA Biotek, China
23225	PierceTM BCA Protein Assay Kit	Thermo Scientific, US

2.1.9. Vectors

Catalog Number	Vector Name	Brand
#49386	pcDNA3 APEX2-NES	Addgene, USA
#1764	pBabePuro	Addgene, USA

#1765	pBabeHygro	Addgene, USA
	pEGFP_N1_TAGLN2	Gift from Prof.Chang-Duk Jun, South Korea
	pBabePuro-Flag-APEX2	Created in house
	pBabePuro-Flag-APEX2-STK10	Created in house
	pBabeHygro-STK10	Created in house

2.1.10. Equipments

Equipment	**Brand**
Centrifuges	Heraeus, Turkey
	Beckman, USA
	Nuve, Turkey
Laminar Flow Hood	Nuaire, USA
CO_2 Incubator	Thermo Scientific, USA
Amersham™ Imager 600	GE Healthcare, USA
Thermocycler	Bio-Rad, USA
Mini-Protean Tetra Cell	Bio-Rad, US
Mini-PROTEAN® gel casting module	Bio-Rad, US
Power supply	Bio-Rad, US
NanoDrop 1000	Thermo Scientific, USA
Vortex	Isolab, Wertheim, Germany
Water bath	Nuve, Turkey
Horizontal shakers	FinePCR, South Korea

Leica Inverted Microscope	Leica Microsystems,Germany
EVOS Cell Imaging Systems	Thermo Scientific, USA
Agarose Gel Electrophoresis System	

2.2. Methods

2.2.1. Cell Culturing

All the cells were maintained in 10 cm plates. The incubations were done under the conditions of 37^{o}C and 5% CO_2. The passaging of the cells was done every 3-4 days. Medium changes were done on non-confluent plates. HMEC cells were split in 1:10 ratio and were maintained in DMEM/F12 supplemented with 1% penicillin/streptomycin, 4% Fetal Bovine Serum (FBS), 1% L-Glutamine, 0.01ng/mL EGF, 25 ng/mL hydrocortisone, 0.025 mg/mL human insulin. HEK293 cells were split in 1:12 ratio as well and they were maintained in high glucose DMEM supplemented with 8% FBS, 1% Non-essential amino acids and 1% P/S.

For thawing the cells, firstly, the vial was heated at 37 ^{o}C until it is completely thaw. The cell mixture was transferred into 5 mL of maintenance media and the falcon was centrifuged at RT at 1500 rpm for 5 minutes. The supernatant was aspirated, the cells were resuspended in growth media and they were put into a 6 cm plate. Incubated in 37^{o}C and 5% CO_2 until confluency. Then, they were transferred into a 10 cm plate by performing splitting protocol.

The splitting protocol was done by aspirating the media on the cells, washing with 5mL 1X PBS (without calcium and magnesium) once, aspirating PBS, adding 1-2 mL 0.05%

trypsin on the cells, incubating 5 minutes at 37ºC and 5% CO_2, inactivating trypsin with the addition of growth media. The protocol continued by transferring the cell suspensions to 15 mL falcon tubes, centrifuging at RT at 1500 rpm for 5 minutes, aspirating the supernatant, resuspending the cell pellet with growth medium, splitting it into plates in 1:10 ratio.

The cells were frozen when needed. The freezing media contained 50% FBS and 10% DMSO in DMEM. 2-3 vials were frozen from a 10 cm plate in 80% confluency. For freezing, Mr. Frosty was used. For long term storage, the vials were stored in liquid nitrogen.

2.2.2. Antibiotic Kill Curve Production

To find out the amount of the Puromycin needed for the selection of HMEC cells, puromycin kill curve experiment was performed. 25.000 HMEC cells per well were seeded in duplicates into the wells of 12 well plates. When the cells were around 50% confluent, puromycin were given to them in increasing concentrations(0, 0.5, 1, 1.25, 1.5, 1.75, 2, 2.5, 3, 5 µg/mL). The cells were checked everyday. Optimal dose for the puromycin was selected as 5 µg/mL for HMEC cells. The cells died 3 days after selection dose was given.

2.2.3. Cloning Experiments

2.2.3.1. Construction of pBabePuro-FLAG-APEX2-STK10 Plasmid

To produce this construct, a two step cloning strategy was employed. The first step was to produce pBabePuro-FLAG-APEX2 plasmid, the second one was to use this plasmid to produce the final product pBabePuro-FLAG-APEX2-STK10 plasmid. This

two step strategy was needed because STK10 ORF can be cut by most of the commercial restriction enzymes.

Firstly,to produce the pBabePuro-FLAG-APEX2 plasmid, the FLAG-APEX2 was amplified by polymerase chain reaction using primers with EcoRI and BamHI cut-sites. The product was purified using O.M.E.G.A PCR purification kit. Then, this purified amplification product and an empty pBabePuro vector was cut with BamHI and EcoRI enzymes. After purification using Thermo Scientific Gel Extraction Kit, the products were ligated together by using NEB T4 DNA Ligase. The ligation product was ran on gel in order to check if the ligation worked or not. After approving that the ligation worked, the ligation product was transformed using C3040I *E.coli* competent cell strain. The transformation products and control were spread on ampicillin containing plates and the day after, 6 colonies were picked from the experimental plate to use for screening. The colonies were grown in LB media containing ampicillin overnight. Thermo MiniPrep Kit was used in order to purify the plasmids of the selected colonies. They were cut with BamHI and EcoRI again and ran on agarose gel to check if some of them contains pBabePuro-FLAG-APEX2 plasmid. The one having the plasmid was selected and a new transformation with *E.coli* was done using the MiniPrep product. A colony was picked from the plate the next day and grew in LB media containing ampicillin and incubated at 37 ^{o}C. From this culture, the cells were amplified and the plasmids were purified by using Qiagen MidiPrep Kit.

For the second part of the cloning strategy, the pBabePuro-FLAG-APEX2 plasmid produced at the first part and pBabeHygro-STK10 vector our lab had before were cut by using SalI-HF enzyme. The cut products were purified either using Thermo Scientific Gel Extraction Kit or O.M.E.G.A PCR purification kit. The purified products were ligated together by using NEB T4 DNA Ligase. The ligation product was ran on

gel in order to check if the ligation worked or not. Again, transformation experiment was performed the same way as the first part of the cloning, and again 6 colonies were picked and screened after DNA isolation by miniprep. This time, the screening was done by cutting the miniprep products with BamHI-HF enzyme. The directionality of the insert was also checked by using BamHI-HF enzyme. From the screened colonies, one colony was selected and the plasmid was amplified and isolated using the same MidiPrep protocol as used before. At the end, pBabePuro-FLAG-APEX2-STK10 plasmid was produced. All of the procedures mentioned above can be found in detail starting from part 2.2.2.1.1.

2.2.3.1.1. Polymerase Chain Reaction for FLAG-APEX2 Amplification

FLAG-APEX2 encoding gene was amplified from pcDNA3-APEX2-NES vector. PCR primers were produced to have BamHI cut-site on forward primer and EcoRI cut-site on reverse primer. The sequences of the primers can be seen on **Table 2.1.** The cut-sites were annotated with uppercase letters. PCR ingredients and the program protocol can be found on **Table 2.2** and **Table 2.3**. . Four 25 µL reactions were ran and they were pooled together at the end of the reaction.

Table 2. 1 Primer sequences to amplify FLAG-APEX2

Direction	**Primer Sequence**
Forward	5’ caagGGATCCgccgccaccatggactacaa 3’
Reverse	5' tccagGAATTCcagctgcagggcatcagcaaa 3'

Table 2. 2 PCR Ingredients for FLAG-APEX2 Amplification

Ingredients	**Volume**
5X Q5 High Fidelity Buffer	5 µL
10 mM dNTPs	0.5 µL
10 µM Forward Primer	1.25 µL
10 µM Reverse Primer	1.25 µL
pcDNA3-APEX2-NES	1 µL (36 ng)
Q5 High Fidelity DNA Polymerase	0.25 µL
DEPC treated water	15.75 µL

Table 2. 3 PCR Program Protocol for FLAG-APEX2 Amplification

Step	**Duration**	**Temperature (ºC)**	**Cycle**
Initial Denaturation	30 seconds	98	-
Denaturation	10 seconds	98	35 Cycles
Annealing	30 seconds	72	
Extension	20 seconds	72	
Final Extension	2 minutes	72	-
Hold	∞	4	-

After PCR reaction, the product was purified by using O.M.E.G.A. PCR Purification Kit. The product was ran on agarose gel to check its integrity and it's concentration was checked using Nanodrop.

2.2.3.1.2. Restriction Enzyme Digestion

The reaction components and the volumes can be seen on **Table 2.4.** Similar reaction was used for every restriction enzyme digestion experiment in this project.

Table 2. 4 Restriction Enzyme Digestion Reactions

	Reaction Volumes for 40 µL reaction
DNA	2 µg (Volume x)
10X CutSmart Buffer	5 µL
Restriction Enzyme	1 µL
DEPC Treated Water	40 µL – (6 + x) µL

The incubation duration was changed according to the enzymes used in the experiment. Generally, 30 minutes to 1 hour 37 ^{o}C incubation was performed. After SalI-HF enzyme cut, since it produces sticky ends, to prevent self-ligation, 2 µL of Shrimp Alkaline Phosphatase was given to the digestion reaction and the tubes were incubated half an hour extra at 37 ^{o}C. The reaction was stopped by doing appropriate heat inactivation according to the enzyme used. After that, the reaction products were purified by performing the protocol of Thermo Scientific Gel Extraction Kit. The concentrations of the purified reaction products were checked by using a Nanodrop.

2.2.3.1.3. Ligation

The purified DNAs were ligated using NEB T4 DNA Ligase. The ligation reaction calculations were done using online tool NEB Ligation Calculator. By using it, 3:1 Insert to vector molar ratio was ensured. The reaction details can be found on **Table 2.5.**

Table 2. 5 Ligation Reaction Components and Their Volumes

	Volume For Ligation Experiment	**Volume For Control Experiment**
Linearized Vector DNA	x µL (100 ng)	x µL (100 ng)
Insert	y µL (3:1 insert to vector ratio)	-
10X T4 DNA Ligase Buffer	2 µL	2 µL
T4 DNA Ligase	1 µL	1 µL
DEPC Treated Water	20 µL – (3 + x + y) µL	20 µL – (3 + y) µL

Ligation was incubated overnight at RT. After incubation, 5 µL of the ligation product was ran on agarose gel to check if the experiment worked or not.

2.2.3.1.4. Bacterial Transformation

C3040I E.coli competent cell strain was used for transformation experiments. 50 µL competent cells were thaw on ice. 10 µL of ligation reaction product or control were given to the cells. (If a previously purified vector was going to be given to the competent cells to be transformed, around 20-30 ng of that plasmid was used.) The cell-DNA mixes are incubated on ice for 30 minutes. After incubation, the cells were heat shocked for 45 seconds in 42 ^{o}C using a waterbath. The tubes were put back on ice for 2 minutes. 950 µL of NEB Outgrowth Media were given to each tube. The tubes were incubated in shaking incubator at 37 ^{o}C for 1 hour. After that, they were centrifuged at 3000 rpm of a standard microcentrifuge for 5 minutes at RT. 900 µL of supernatants were taken. The pellets were dissolved in the remaining supernatant and this was spread onto ampicillin containing LB-Agar plates and incubated overnight at 37 ^{o}C.

2.2.3.1.5. Screening and Selecting Transformation Products

Some colonies were picked from a previously spread plate. The pickings were done by taking a colony with a sterile 200 µL tip and putting the tip inside a round bottom tube containing 3 mL LB with ampicillin. This media with colony was incubated in a shaker overnight at 37 ^{o}C. After 16 hours of incubation, the LB with grown cells were centrifuged at 3000 rpm for 5 minutes at RT for pelleting. The protocol for Thermo Scientific MiniPrep was used to isolate the plasmid DNA from them. Then, the MiniPrep products were cut with the appropriate restriction enzymes and ran on agarose gel. The predicted banding pattern was checked for each product. One of the selected colonies having the predicted pattern was selected. Transformation experiment was carried out using this plasmid. A single colony was grown in LB ampicillin media and amplified performing Thermo Scientific MidiPrep protocol.

2.2.3.1.6. Agarose Gel Electrophoresis

Needed amount of agarose was weighted using a precision scale. In general, 1% gel was made. For this, 1g of agarose was added to 100 mL of 1X TAE buffer in a flask. This mixture was heated for 2 minutes at the highest power of a standard microwave. After microwave, the mixture was cooled in room temperature. When it is cooled to be touched, 3-5 µL of Ethidium Bromide was added to the mixture and it was shaken for it to be mixed properly. Then, the melted gel with ethidium bromide was poured into a gel casting tray and the appropriate comb was put on top of the melted gel. After solidification, the comb was taken out. The gel was put inside the agarose gel tank and the tank was filled with 1X TAE. The DNA to be loaded were mixed with DNA loading dye and they were loaded to the wells of the gel. The gel was ran at 100V until

the dye front reaches more than half of the gel. The imaging of the gels was done with agarose gel imaging system.

2.2.4. Vector Transfections

2.2.4.1 Calcium Phosphate Transfection

Calcium phosphate transfection protocol was adapted from the protocol of Kingston & Okayama [25].

First, the chemicals needed for the protocol were made. 2.5 M $CalCl_2$ was made by dissolving 18.37 g of $CaCl_2.2H_2O$ in 50 mL sterile water and filtered through a 0.45 µM filter to sterilize. 2X HEPES Buffered Saline (HeBS) buffer was prepared by adding 818.16 mg of NaCl, 595.75 mg of HEPES and 13.349 mg of $Na_2HPO_4.2.H_2O$ into 40 mL of sterile water. This solution was titrated with 5N NaOH to have pH=7.04. The solution was then filter sterilized. Aliquoted solutions were stored in -20 ^oC.

Confluent HEK293 cells in 10 cm plates were splitted 1/12 in 10 cm plates a day before the experiment. On the day of the experiment, 2 hours before the transfection, the media of the cells were replenished with 9 mL complete media. A solution containing 10 µg Plasmid DNA to be transfected and sterile water was prepared by adding 10-15 µg DNA in a tube and topping it with the sterile water up to 450 µL. then, 50 µL $CaCl_2$ was added into this mixture. 500 µL 2X HeBS was added into a 15 mL falcon tube. A pipettor with 2 mL pipet was used to bubble this solution and then the DNA/$CaCl_2$ solution was added to this solution dropwise. The mixture was vortexed immediately and allowed to sit 20 minutes at room temperature. After the 20 minutes, the solution was distributed evenly on the cells seeded on the previous day. The plates were shaken slowly to mix the media. The cells were then incubated at 37^oC and 5% CO_2 for 16 hours. After 16 hours, the media were discarded and the cells were washed with

1X PBS 2 times, then normal media were given to the cells. In total, 48 or 72 days of incubation were done before scraping the cells according to the experiment. Then, the cells were scraped and lysed to get whole protein lysate.

2.2.4.2. Producing Stable Cell Lines

2.2.4.2.1. Lipofectamine Transfection

Viral particles were produced using Lipofectamine 3000™ for transfection part. First, 200.000 HEK293 cells were seeded onto 4 wells of a 6 well plate using maintenance media containing 8% FBS in High glucose DMEM. After a day (Day 2), the when the cells were 70-80% confluent, Lipofectamine 3000™ protocol was performed. Two solutions were prepared in Tube A and Tube B for each well. Tube A contained 125 µL DMEM, 3.75 µL Lipofectamine 3000™. Tube B contained 125 µL DMEM, 2.5 µg DNA, 5 µL P3000™. DNA inside Tube B contained 2:1:1 ratio (vector to be used : gag/pol : vsv.g respectively) of the µgs of the DNAs needed to produce viral particles. Tube A and B were mixed and incubated at RT for 10-15 minutes. After incubation, The mixture was given to a well drop by drop. This was done for all of the wells. The day after (Day 3), the media was aspirated and refreshed with maintenance media. On Day 4, media was collected from the wells and put in a falcon covered with aluminum foil, stored at +4 degrees. Media of the wells were refreshed. On Day 5, Supernatant was collected in the same falcon as the day before and filtered with 0.45 micron filter. It was again put in +4 degrees until used for retroviral transduction part (Can be stored up to a week).

2.2.4.2.2. Retroviral Transduction

The cells were seeded on 6 well plate wells. The number of cells will be seeded changes from cell line to cell line, for HMEC cells, 40.000 cells were seeded per well.

The day after, cells were around 20% confluent (It must be noted that the confluency should not be more than this for optimal conditions). 1 volume of Lenti-X concentrator with 3 volumes of clarified and filtered supernatant were mixed by gentle inversion. It was incubated in +4 degrees for 30 minutes – overnight. Then, the mixture was centrifuged at 1500g in a falcon centrifuge for 45 minutes at +4 ^{o}C. A whiteish pellet was observed after the centrifuge. The supernatant was removed, the pellet was resuspended in 2 mL maintenance media. This suspension was given to the transduction well. 10 µg/mL polybrene was given to each well. The day after, medium was changed (If the cells were confluent this day, passage was done). The next day, selection dose of the antibiotic was given. The selection well was checked until control cells die completely. After the selection was done, maintenance dose of the antibiotic (around 1:4th of the selection dose) was routinely given to the cells.

2.2.5. Protein Biochemistry

2.2.5.1. Cell Harvesting and Lysis

The media were removed from cells and they were washed in 1X room temperature PBS once. Then, PBS were discarded. 5 mL of 1X ice cold PBS were given to the each plate. Afterwards, to remove the cells from the plates, scraping was performed. The cells were transferred to 15 mL Falcon tubes and centrifuged at 1500 rpm for 8 minutes at 4°C. The supernatant were discarded. Then, the pellet was snap-frozen in liquid nitrogen and stored at -80°C.

The appropriate lysis buffer was made and stored on ice until right before the cells were lysed. Lysis buffer (RIPA or NP40) were added to the pellet (1:1 buffer to lysate ratio for RIPA, 2:1 for NP40). NP40 based buffer was used for Co-IP protocols in order to preserve protein-protein interactions better. Afterwards, the pellets in lysis buffer

were incubated on ice for 30 minutes. In every 10 minutes, the pellets were flicked in order to dissolve in lysis buffer. After the incubation, the mixtures were centrifuged at 4 degrees Celsius for 15 minutes at 13000 revolutions per minute. The pellets were thrown away and the supernatant was collected in fresh eppendorf tubes. Long-term storage of the lysates was achieved at -80°C after being snap-frozen in liquid nitrogen.

This protocol was used for regular western blotting experiments. For producing lysates for the mass spectrometry analysis, another protocol was used, it can be found at part 2.2.3.4.

2.2.5.2. Protein Quantification by Bradford Assay

The protein concentrations of the lysates were quantified by performing the manufacturer's protocol (Pierce™ Coomassie Plus (Bradford) Assay Kit). Standards were prepared by diluting 2mg/mL BSA solution. The standard concentrations are shown in the **Table 2.6**. Protein lysates were diluted 1/10 with autoclaved ddH_2O. After dilution, 5 µL of each diluted lysate were loaded into the wells of a 96 well plate in triplicates. 250 µL of Coomassie Blue dye were given to each well and the plate was mixed for 30 seconds. Then, it was incubated for 10 minutes in dark at room temperature. After that, the measurement was done at 595 nm using a spectrophotometer.

Table 2. 6 Standard preparation for Bradford Assay

Standard	Protein amount (µg)	2mg/mL BSA used (µL)	Autoclaved ddH2O used (µL)
A	10	300	0
B	7.5	375	125
C	5	325	325
D	3.75	175 from B	175
E	2.5	325 from C	325
F	1.25	325 from E	325
G	0.625	325 from F	325
H	0.125	100 from G	400
I	0	0	400

The concentrations of the samples were then retrieved by doing the calculations on the standard curve. The absorbance values of each sample were used to quantify the concentration of the proteins inside.

2.2.5.3. Western Blotting

Protein amounts to be put in each well was calculated after Bradford Assay. The protein samples were prepared using 1x Laemmli Buffer as the loading buffer. 15-20 µg of proteins were loaded to the wells according to the experiment.

To perform Sodium Dodecyl Sulfate Polyacrylamide Gel Electrophoresis (SDS-PAGE), polyacrylamide gels were hand cast by using the recipe seen in **Table 2.7**. 10% resolving gel and 4% stacking gel were used. 1.5 mm separating glasses and Mini Protean Gel Casting system was used to cast the gels.

Table 2. 7 Resolving and Stacking Gel Recipes for SDS-PAGE

Ingredient	**10% Resolving Gel**	**4% Stacking Gel**
Acrylamide/bisacrylamide (30% w/v)	3.3 mL	0.66 mL
ddH2O	4.1 mL	3 mL
Resolving Gel Buffer (pH=8.8)	2.5 mL	-
Stacking Gel Buffer (pH=6.8)	-	1.26 mL
10% APS	50 µL	25 µL
TEMED	5 µL	5 µL

The gels were run at constant 100 volt around 90 minutes until the dye front leaves the gel. After running, the proteins were transferred to nitrocellulose membranes by performing wet transfer. The transfers were done at constant 250 mA for 150 minutes. The transfers were done on ice in order to prevent overheating. To check the transfer efficiency, the membranes were stained with Ponceu S stain. The membranes were washed with distilled water to get rid of the excess stain. Then, they were cut accordingly in order to check multiple proteins in one membrane. The membranes were blocked in 5% Milk or BSA by incubating on a shaker for 1 hour at RT. After blocking, primary antibodies (Generally 1:1000 dilution in 3% BSA) were given to membranes and they were incubated on a shaker overnight at +4 ^{o}C. After the incubation, the primary antibodies were taken out from them and they were washed with 1 X TBS-T on a shaker at RT for 5 minutes three times. According to the primary antibodies, HRP conjugated mouse or rabbit secondary antibodies (1:10000 in 3% BSA solution) were given to the membranes. They were incubated on a shaker for 1 hour at RT. After that, the secondary antibodies were taken out from them, and they were washed with 1X TBS-T on a shaker at RT for 5 minutes three times. The membranes then were incubated in ECL solution for a minute or so. The excess ECL

were taken from them by using a tissue paper. Imaging of the membranes were done with Amersham Imager 600.

2.2.6. Proximity Based Biotinylation

We used a modified version of the protocol used by Tan et. Al., [26]. The compositions of the solutions and the buffers used in this experiment can be found in the Materials part. Firstly, Biotinyl Tyramide treatment of the cells were done. HMEC-FLAG-APEX2-STK10 cells were passaged in 10 cm plates to be confluent on the experiment day. For treating one plate, Biotinyl Tyramide was added to 5 mL warm growth medium in a falcon tube to a final concentration of 0.5 mM and it was mixed well. The medium in tissue culture dishes were replaced with medium supplemented with 0.5 mM Biotinyl Tyramide. Cells were placed back into the incubator set to 37 ^{o}C, 5% CO_2 and incubated for 2 hours. While incubating, the pre-weighed quenchers were dissolved and mixed into the lysis buffer and Quenching buffers. Just before using, fresh 1mM H_2O_2 was prepared by diluting 10M stock in PBS^{++}. This solution was cooled by putting it on ice. It is important to prepare the chemicals just before use for them not to lose their activity. After the incubation time was over, Biotinyl Tyramide containing media was aspirated from the plate. It was washed three times with PBS^{++}. The PBS^{++} was aspirated and 1mM H_2O_2 was added onto the cells. The plate was incubated at RT for exactly 2 minutes. The incubation time was monitored strictly in this experiment since even seconds may cause extra biotinylation in the cells. After incubation, H_2O_2 containing buffer was aspirated and the activity of H_2O_2 was stopped using quenching buffer. The cells were washed with quenching buffer three times. Afterwards, 500 µL lysis buffer containing the quenchers was given to the plate. They were scraped on ice, transferred in a 1.5 mL Eppendorf tube. For the samples sent to the mass spectrometry analysis, two plates were pooled into one Eppendorf tube (As negative

control, cells without H_2O_2 were used). Afterwards, the cells in lysis buffer were incubated on ice for 30 minutes. After the incubation, the experiment was paused by snap freezing the lysate with liquid nitrogen and storing in -80 ^oC. A day after, the frozen lysate was thawed on ice and it was sonicated in a bath sonicator on medium intensity (Amplitude of 40%) for 30 seconds, paused 30 seconds, and this was repeated once. The lysate was cleared by centrifuging at 20,000 x g for 30 minutes at 4 ^oC. The supernatant containing the proteins was collected and the pellet was disposed. 50 µL of the lysate was stored for using it as the input for the pull-down experiment. 35 µL of the lysate was stored to be quantified with Bradford Assay.

2.2.7. Streptavidin Pull-Down

The compositions of the solutions and the buffers used in this experiment can be found in the Materials part. All the centrifugations in this protocol was done at 3000 rpm of a standard microcentrifuge for 2 minutes at 4 ^oC.

1mL RIPA buffer was added to 40 µL of Streptavidin Sepharose beads (Not the harm the beads, the pipette tip to be used to take the beads was cut with a clean razor), it was centrifuged, the RIPA buffer was discarded. 1 mL RIPA was added onto the beads again, it was washed by inversion. This wash was repeated once. The RIPA was removed, and clarified cell lysate was added to the equilibrated Sepharose beads. The samples were incubated on a rotating wheel for 4 hours at 4 ^oC. After incubation, the lysate-bead mixture was centrifuged, the supernatant was discarded, 1 mL RIPA was added on top of the beads. It was inverted for 2 minutes with the help of a rotating wheel. The mixture was centrifuged, the supernatant was discarded, 1 mL 1M KCl was added on top of the beads. It was inverted for 2 minutes. The mixture was centrifuged, the supernatant was discarded. 1 mL 0.1 M Na_2CO_3 was added onto the beads, it was

inverted it for 2 minutes. The mixture was centrifuged, the supernatant was discarded. 1 mL 2 M Urea in 10 mM Tris-HCl (pH:8) was added onto the beads and it was inverted it for 2 minutes. The mixture was centrifuged, the supernatant was discarded.1mL RIPA was added onto the beads and it was inverted for 2 minutes. The mixture was centrifuged, the supernatant was discarded. 1 mL PBS^{++} was added onto the beads and inverted for 2 minutes. (The samples to be sent to mass spectrometry were put in a packaging with cooling packs at this step and sent to the mass spectrometry facility. The elution step was done at the facility by the researchers there.)

Elution protocol for western blotting analysis (This protocol was performed in our lab to analyze the pulled down proteins): The mixture was centrifuged, the supernatant was discarded, the beads were centrifuged again, supernatant was removed as much as possible using a 20 µL tip. 80 µL of elution buffer was added onto the beads. The beads were incubated at 95 ^{o}C for 15 minutes. It was centrifuged at RT for 2 minutes.

The supernatant was transferred to a fresh tube and it was analyzed by performing western blotting with it.

2.2.8.Co-Immunoprecipitation

All of the centrifugations done in this protocol were performed at 3000 rpm of a standard microcentrifuge at +4 ^{o}C for 5 minutes. The cells were lysed using NP-40 based lysis buffer by performing lysis protocol in part 2.2.5.1. After quantification, 1-2 mg protein in 500 µL lysis buffer was used for immunoprecipitation. To preclear the protein lysates, 20 µL of protein A/G agarose bead slurry was added to 500 µL NP-40 lysis buffer. The beads were centrifuged and the supernatant was discarded. The protein lysate was added on top of the beads and the mixture was incubated on a rotating wheel at +4 ^{o}C for 30 minutes. The mixture was spun again after the

incubation, the supernatant containing cleared lysate was collected and the beads were discarded. The primary antibody that would be used for the pull down was added into the cleared lysate in the suggested concentration. For negative control, either empty beads or random rabbit Igg's were used. The antibody-protein mixture was incubated overnight at +4 ^{o}C in an ice box. After incubation, 50 µL of protein A/G agarose bead slurry was added to 500 µL NP-40 lysis buffer. Then they were spun, and the supernatant was discarded. The antibody-lysate mixture was added onto the equilibrated beads. This mixture was incubated on a rotating wheel at +4 ^{o}C for 2 hours. The mixture was spun and the supernatant was discarded, the beads were collected. Then the beads were washed with 500 µL NP-40 lysis buffer. They were spun and the supernatant was discarded. This was repeated three times. After washing steps, 30 µL laemmli buffer based elution buffer containing beta-mercaptoethanol was added to the beads. This mixture was boiled for 15 minutes at 95 ^{o}C. Then it was spun at 3000 rpm at room temperature. The supernatant containing the eluted proteins were collected and they were used in the subsequent western blotting experiment. The co immunoprecipitated proteins were checked by probing the membrane with the specific primary antibody of the protein of interest.

2.2.9. Immunofluorescence Experiments

50.000 HMEC-APEX2-STK10 cells were seeded onto coverslips in a 35 mm cell culture dish. A day after, the cells were transfected with 4 µg eGFP-TAGLN2 plasmid using Lipofectamine 3000. The immunofluorescence experiment was performed after 48 hours of transfection. The supernatant was aspirated. Then, the cells were fixed by using fixation solution (4% PFA in PBS). 1mL fixation solution was added onto the slides and they were incubated at 15 minutes in dark. The slides were washed with PBS two times after the incubation. The washing was performed by adding PBS onto

the slides and incubating them with PBS for 5 minutes, then discarding the PBS. To permeabilize the cells, the cells were incubated with 0.5% Triton X in PBS fpr 10 minutes in dark. After the permeabilization, the cells were washed with PBS two times. For blocking, 10% BSA in PBS was used, this solution was added onto the slides and they were incubated for 30 minutes at room temperature. The primary antibody (FLAG antibody) was diluted in 3% BSA containing PBS solution in 1:1000. 200 µL of primary antibody solution was added onto the slides. The slides were incubated at room temperature in dark for 2 hours. After the primary antibody incubation, the slides were washed with PBS for 5 minutes three times. Then they were incubated with secondary antibody conjugated to RFP. 200 µL of 5µg/mL secondary antibody was used and the slides were incubated for 45 minutes. After incubation, the slides were washed with PBS for 5 minutes three times. The slides were dried using tissue paper and they were mounted on slide using 10 µL of mounting media containing DAPI. The slides were sealed with nail polish. The imaging of the slides was done using Evos immunofluorescence microscope. For the quantification, ImageJ JaCoP Plugin was used, correlation results were obtained. The cells having GFP and RFP signals were counted manually, the number of cells having co-localization were used to plot bar graphs. GraphPad Prism was used to plot the graph and perform student t-test.

2.2.10. LC-Mass Spectrometry

This part of the experiment was done by our collaborators from Prof.Dr. Nurhan Özlü's lab at the Koç University Proteomics Facility (KUPAM), Istanbul, Turkey. Each sample underwent on-bead tryptic digestion for mass spectrometry protein identification. Protein-bead complexes were washed with 8 M urea in 0.1 M Tris-HCl pH 8.5 solution, reduced with 100 mM DTT in urea solution at 56°C for 45 minutes, and alkylated with 50 mM chloroiodoacetamide at room temperature for 30 minutes. For the removal of

the urea solution, the beads were washed with ammonium bicarbonate solution (50 mM NH_4CO_3). Beads were digested overnight at 37°C with 4 µg of trypsin (Sigma catalog no: T1426) for 600 µg of protein. Peptides were desalted and eluted using C18 cartridges after 10% formic acid stopped trypsin digestion. Eluates were dried using a speed vacuum system (Thermo Fisher Scientific cat no: SPD1010) and analyzed using a C18 nanoflow reversed-phase Dionex Ultimate 3000RSL liquid chromatography (LC) system with Q-Exactive Orbitrap mass spectrometer (MS/MS). Samples were separated on a packed 75 µm i.d. × 40 cm C18 column (Reprosil-Pur C18, 1.9 µm, 200 Å, Dr.Maisch) using 100 min linear gradients from 5 to 40% acetonitrile in 0.1% formic acid with 300nL/min flow in 120 minutes. MS1 spectrum (Orbitrap analysis; resolution 70000; mass range 400−1500 m/z; AGC target 3e6; maximum injection time 60 ms) started the scan sequence. Up to 15 of the most intense ions per cycle were fragmented and analyzed in the Orbitrap with data-dependent acquisition (DDA). MS2 analysis used collision-induced dissociation (HCD) (resolution 17500; AGC 1e6; NCE26; maximum injection time 100 ms). The isolation window for MS/MS was 2.0 m/z. The data was searched against the human UNI-PROT 2016 database. Thermo Proteome Discoverer 2.3 used Sequest HT and Mascot to identify proteins in raw files. Acetylation (protein N-termini) and methionine oxidation were variable modifications, while cysteine carbamidomethylation was fixed. Two missed cleavages maximum was allowed for the tryptic peptides. The precursor mass tolerance was set to 10 ppm, and both peptide and protein false discovery rates (FDRs) were set to 0.01.

2.2.11. Bioinformatical Analysis

2.2.11.1. Selection of the Candidate Proteins

Our collaborators sent us the protein list they analyzed as explained in 2.2.8. For the experiment, we had two biological replicates and a negative control which was the experimental product without H_2O_2 treatment. Each sample were ran through mass spectrometry three times and we had the protein results from each read as separate files. Firstly, using Microsoft Excel filters, the proteins which were read at least 2 times in 3 reads were selected in each sample. Then, from each experimental replica list, the proteins found also in negative control were deleted. From this analysis, 16 proteins were selected. Also, for more comprehensive analysis, another list was made by adding the proteins only found in one experimental sample to the 16 proteins list. This list had 44 proteins in total. Most analyses were done using the 16 protein list.

2.2.11.2. STRING Analysis

The lists of proteins were put in STRING multiple protein analyzer and the results were downloaded from the website. All of the analyses were done in medium confidence[27].

2.2.11.3. cBioPortal Analysis

cBioPortal Co-Expression analysis was performed to check the possible interaction of STK10 and our candidate proteins[28], [29]. First, Breast Invasive Carcinoma (TCGA, Firehose Legacy) study was selected. Then the needed subtypes of breast cancer were manually selected. Most of the analyses we did were performed with HER2, PR and ER negative (Triple Negative) breast cancers. Then, we put our list of proteins and STK10 in the query in the selected subtype of breast cancer. We analyzed the co-

expression of the proteins with STK10 by selecting the “Plots”. mRNA expression (RNA Seq V2 RSEM) database was selected. STK10 was selected for the horizontal axis, and the candidate protein was selected for the vertical axis. Log scale was selected for both of the proteins.

2.2.11.4. Km Plotter Analysis

For the survival analyses, we used online Kaplan-Meier Plotter[30]. We either used RNA-Seq or Gene-Chip databases for breast cancer. We manually selected TNBC subtype by selecting HER2, PR and ER negative breast cancers. We used multiple gene option and selected the samples with high STK10 expression, then checked the if the candidate protein expression was changing the survival of the patients. For the analysis, auto cut-off or median cut-off were selected. The Km Plots produced were downloaded.

2.2.11.5. Gene Onthology Analysis

For this analysis we used online PANTHER [31] and g:Profiler [32] tools. For both analysis, the proteins found in either one of the replicates were used. In PANTHER analysis, we selected “Protein Class” graph. For g:Profiler analysis, we performed g:GOSt functional profiling and selected the “Detailed Results”tab.

2.2.11.6. Reactome Analysis

We used the proteins found in either one of the replicates for this analysis. We put our list of proteins in the Reactome gene list analysis tool and selected “Project to human”. Then we checked the pathways associated with the STK10 interactome list we had and downloaded the table produced by Reactome [33].

3. RESULTS

3.1. Production of Plasmid Encoding the Fusion Protein

For the biotinylation of STK10, we needed to produce a plasmid encoding STK10 fused with APEX2. To do this, we performed a series of molecular cloning experiments. First, we produced a plasmid encoding APEX2 with pBabePuro backbone. We amplified FLAG tagged APEX2 from commercially available pcDNA3 APEX2-NES vector by performing PCR amplification **(Figure 3.1A)**. We designed a forward primer having a BamHI cut-site and a reverse primer having EcoRI cut-site for this purpose. We cut the amplified FLAG-APEX2 and an empty pBabePuro vector with EcoRI and BamHI restriction enzymes **(Figure 3.1B)** and ligated them together to produce pBabePuro-FLAG-APEX2 plasmid**(Figure 3.1C-D)**.

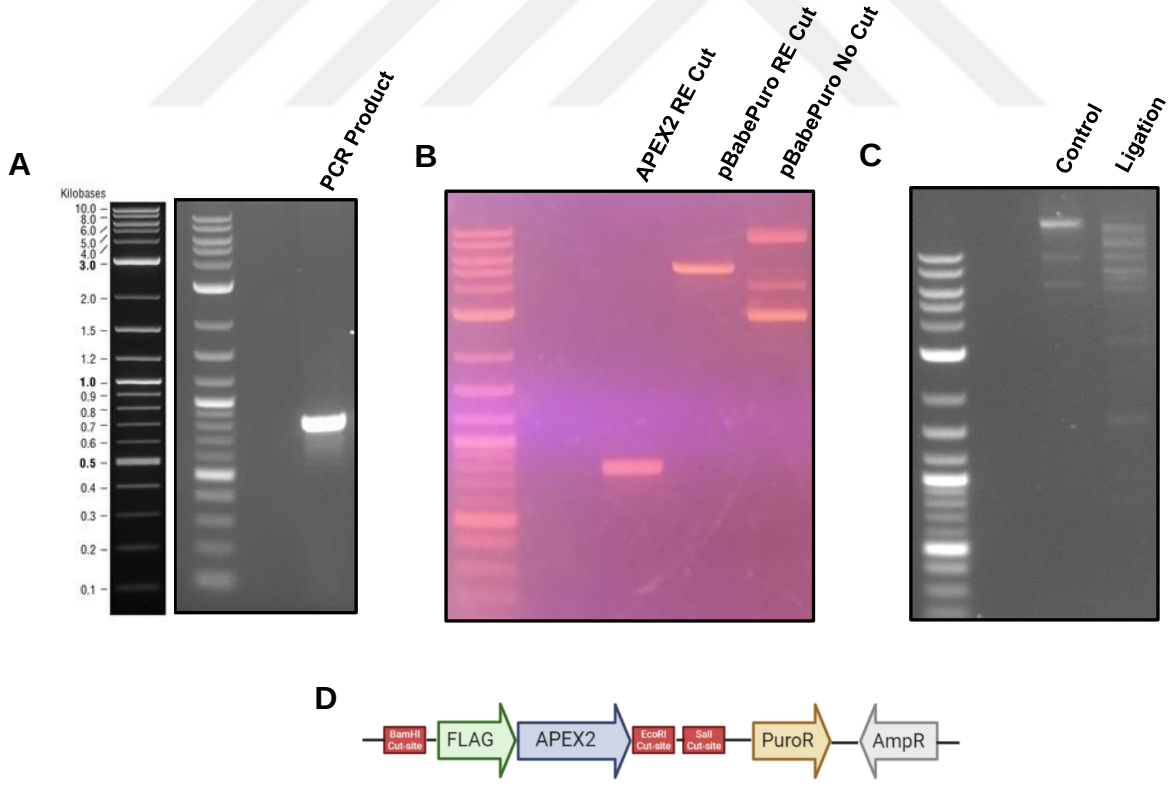

Figure 3. 1 Production of pBabePuro Plasmid Encoding APEX2. A. Agarose gel electrophoresis result after PCR of APEX2 with EcoRI and BamHI restriction sites. **B.** Agarose gel electrophoresis result after the restriction enzyme cut of the PCR product and the empty pBabePuro vector with EcoRI and BamHI. **C.** Agarose gel electrophoresis result after ligation. For control, cut pBabePuro vector without insert was used. **D.** The schematic representation of the produced vector pBabePuro-Flag-APEX2 (Created with Biorender).

After production of this plasmid, we cut both this plasmid and the pBabeHygro-STK10 plasmid produced in our lab before with SalI-HF enzyme**(Figure 3.2A-B)**. By performing gel extraction protocol, we isolated specifically SalI cut STK10. Then, ligated the isolated STK10 sequence with the cut pBabePuro-FLAG-APEX2 enzyme **(Figure 3.2C)**. Then we performed a bacterial transformation experiment with this plasmid and selected six colonies. We purified the plasmid DNA from these colonies and we screened them by performing restriction enzyme cuttings with BamHI enzyme. By doing so, we selected the plasmid having STK10 in the right orientation.

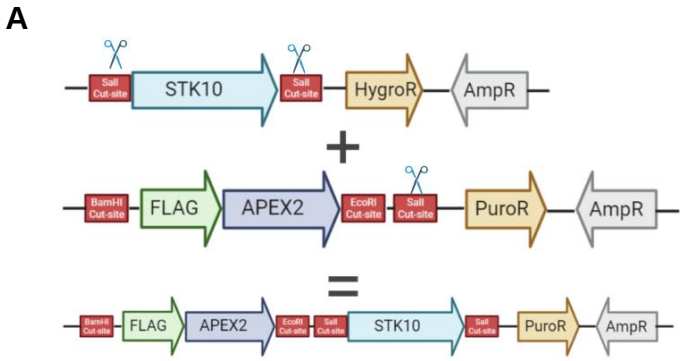

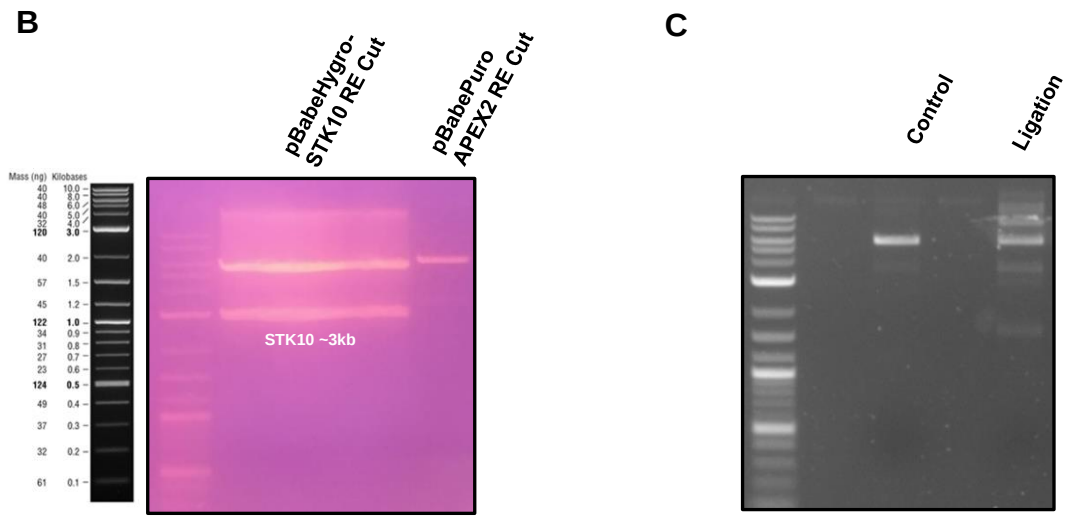

Figure 3. 2 Production of the plasmid encoding the fusion protein. A. The schematic representation of the cloning strategy(Created by Biorender). **B.** Agarose gel electrophoresis result after the restriction enzyme cut of the pBabeHygro-STK10 and pBabePuro-Flag-APEX2 vectors with SalI enzyme. The DNA particles at 3 kB were purified with gel extraction. **C.** Agarose gel electrophoresis result after ligation. For control, cut pBabePuro-Flag-APEX2 vector without insert (STK10) was used.

3.2. Validation of the Fusion Protein Synthesis

To validate the expression of the APEX2-STK10 fusion protein, we performed transient transfection experiment on HEK293 cells with pBabePuro-FLAG-APEX2-STK10 plasmid. After doing western blot, we saw the APEX2 fused STK10 at the expected size. WT STK10 gives signal around 140 kDa and FLAG-APEX2 is around 30 kDa. So, we were expecting to see a 30 kDa upshift in the samples which were transfected with our plasmid. As seen in **Figure 3.3**, we successfully produced the construct with the expected size. Also, to show that the APEX2 fused STK10 is still functioning, we checked p-ERM levels in the cells. STK10 is known to phosphorylated ERM proteins so we wanted to see an upregulation in pERM levels in APEX2-STK10

overexpressed cells and we saw what we expected with our results. So, after this experiment, we confirmed that our fusion protein is at the expected size and STK10 is functioning properly.

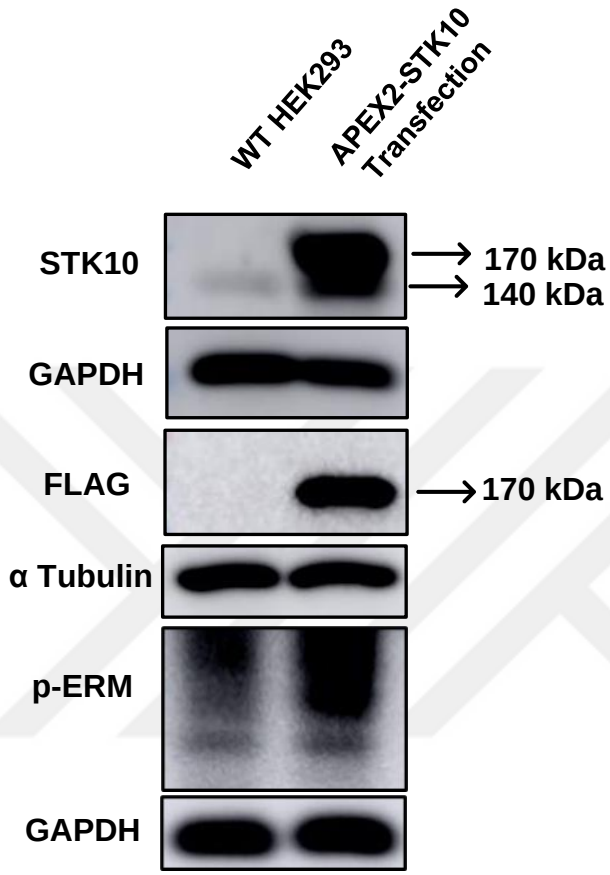

Figure 3. 3 Validation of the Fusion Protein Synthesis. Western blotting results. HEK293 cells were transfected with pBabePuro-Flag-APEX2-STK10 vector using Lipofectamine 3000. The cells were harvested after 48 hours of transfection.

3.3. Producing APEX2-STK10 Expressing Stable Cell Line

We wanted to produce a cell line stably expressing the fusion protein APEX2-STK10. We wanted to find STK10's interaction partners in normal breast cells instead of cancer cells. Because cancer cells have so much heterogeneity between each other, we could have ended up with a complicated interactome. Our group's previous work

showed that STK10 is more effective in triple negative breast cancer subtype, compared to other subtypes. The bioinformatics analyses done by our group before showed that STK10 is mostly expressed in TNBC cell lines. Also, our group's previous wet lab experiments showed STK10 knock-down sensitizing TNBC cell lines to p110α inhibitor BYL-719.

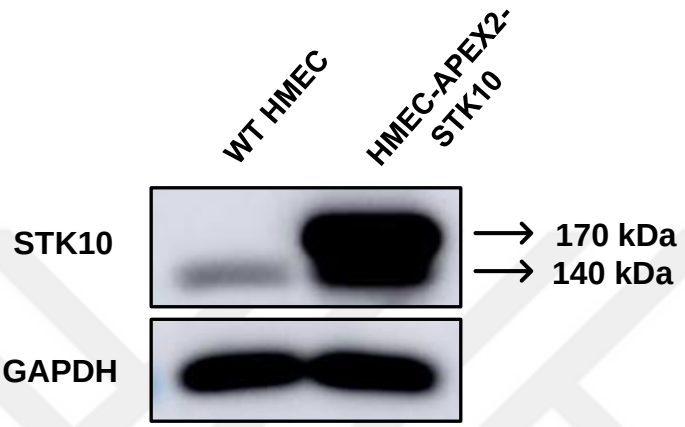

Figure 3. 4 Production of APEX2-STK10 Expressing Stable Cell Line. Western blotting results. Immortalized HMEC cells were retrovirally transduced with pBabePuro-Flag-APEX2-STK10 plasmid.

That is why, we wanted to use a normal breast cell line having similar properties as TNBC. For this purpose, we used immortalized Human Mammary Epithelial Cells (HMEC). We performed retroviral transduction experiment on HMEC cells using pBabePuro-FLAG-APEX2-STK10 plasmid and produced HMEC-APEX2-STK10(HMEC-A-S) cell line. The protein lysates were collected from control and transduced cells. These protein levels of STK10 in both lysates were checked with western blotting **(Figure 3.4)**. We saw the expected up-shift in the STK10 of the newly produced HMEC-A-S cell line. So, we decided to use this cell line for the proximity biotinylation experiment.

3.4. Optimization Of Biotinylation Conditions

For the proximity based biotinylation experiment, we used a modified version of the protocol of Tan et.al. [26]. First, we tried to use the suggested protocol. We performed the experiment with 0.5 mM biotin phenol and 1mM of H_2O_2 on HMEC-A-S cell line. We incubated the cells with biotin phenol for 1 hour and afterwards with H_2O_2 for 1 minute **(Figure 3.5A)**. Also, we performed the same experiment without using either biotin phenol or H_2O_2 . We performed western blot experiment with these protein lysates and checked the membrane with HRP conjugated streptavidin. We expected to see endogenously biotinylated proteins at 75 kda and 130 kda in all of the samples. More importantly, we wanted to see a smeary lane only for the experimental lane with the sample which has been treated with both H_2O_2 and biotin phenol.

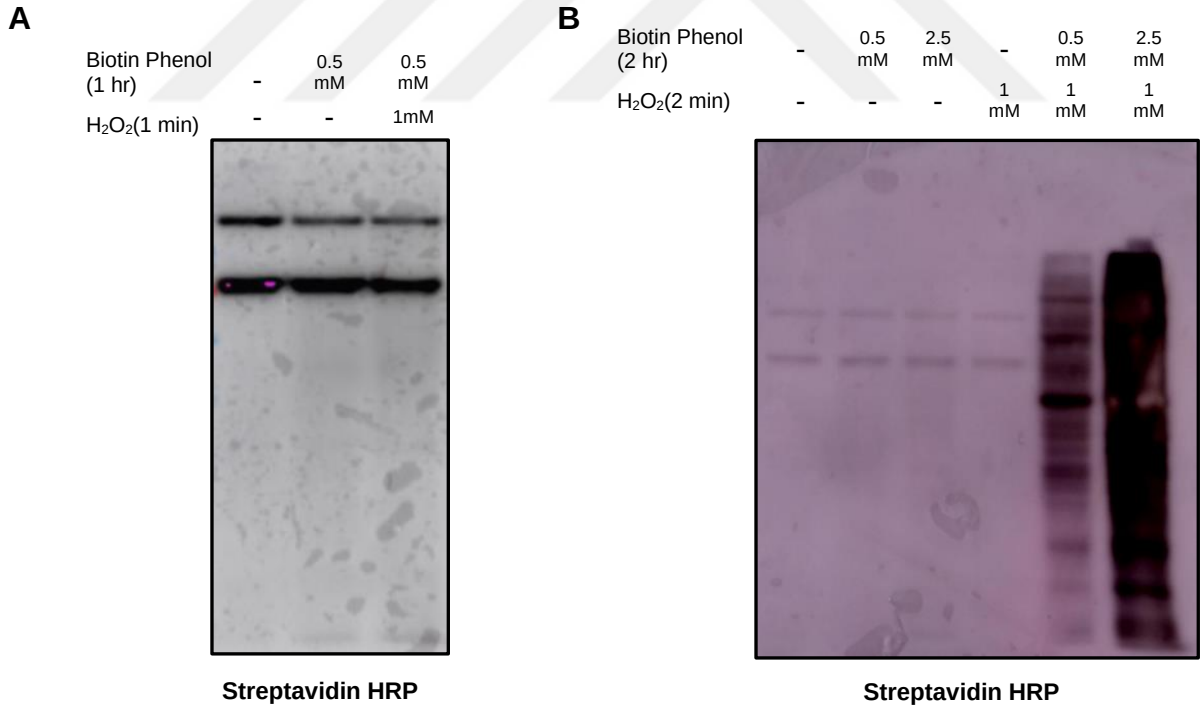

Figure 3. 5 Optimization Of Biotinylation Conditions. Western blot results after incubation with Strptavidin HRP. **A.** Biotinylation check after 1 hour 0.5 mM Biotin phenol and 1 minute 1mM H_2O_2 incubation. **B.** Biotinylation check after 2 hours of different concentrations of biotin phenol incubation followed by 2 minutes of 1mM H_2O_2 incubation.

We were able to see the endogenously biotinylated proteins in all of the samples but we could not see the proteins biotinylated by APEX2 with these experimental conditions. Because of this, we performed an optimization experiment in order to find the optimal amounts of biotin phenol and the optimal incubation time for the biotinylation to occur properly. For this experiment, we increased the incubation times with biotin phenol and H_2O_2. We incubated the cells with biotin phenol for 2 hours and H_2O_2 for 2 minutes. Also, we titrated the biotin phenol in order to find the optimal concentration of it **(Figure 3.5B)**. We were able achieve our desired level of biotinylation when we used 0.5 mM biotin phenol and 1mM H_2O_2. More concentrated biotin phenol treatment resulted in non-specific biotinylation. So, we decided to perform our further experiments with 0.5mM biotin phenol.

3.5. Streptavidin Pull-Down

After optimizing the conditions, we performed streptavidin pull-down experiments to check if we were able to pull down our biotinylated proteins. We performed a western blotting experiment with the eluate and we incubated the membrane with streptavidin-HRP in order to see the biotinylated proteins **(Figure 3.6)**. With this experiment, we showed that we successfully pulled down and eluted the biotinylated proteins.

Figure 3. 6 Streptavidin Pull-Down After Biotinylation. Results after streptavidin pull-down followed by western blotting and Strptavidin HRP incubation.

3.6. Mass Spectrometry Results

We performed new sets of biotinylation and pull-down experiments with the protocols we optimized. We used two biological replicates and one negative control for the experiment. As negative control, we used a sample without H_2O_2 incubation. We sent the pulled down proteins to the mass spectrometry facility on bead and they performed elution and mass spectrometry steps. They analyzed the raw data and sent us lists of proteins. As candidate proteins, we selected the ones found in both of the replicates but not in negative control **(Figure 3.7A-B)**. We also had another more comprehensive protein list with the proteins found in either of the replicates but not in negative control **(Figure 3.7C)**.

A

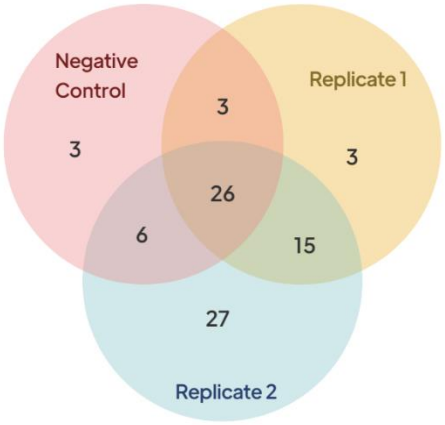

B

First 15 Candidate Proteins				
	Mascot Score	MW(kDa)	Unique Peptides	Coverage (%)
ANXA2P2	259	38.6	4	15
HNRNPK	226	50.9	2	6
YWHAQ	197	27.7	2	12
UBE2L3	148	17.9	1	14
EIF4A1	139	46.1	1	3
MAP4	138	120.9	1	2
PRDX6	125	25	2	12
UBA52	121	14.7	1	7
KRT14	120	51.5	2	6
KPNB1	98	97.1	1	1
EEF1G	78	50.1	1	2
TAGLN2	71	22.4	2	11
FARSB	57	66.1	1	2
ECM29	24	204.2	1	0
TYK2	0	133.6	1	1

C

Proteins found in only one replicate				
	Mascot Score	MW(kDa)	Unique Peptides	Coverage (%)
TUBA4A	519	49.9	1	6
PKM	246	57.9	3	7
UBA1	218	117.8	2	4
DHX15	185	90.9	1	2
LDHA	139	36.7	1	5
EEF2	122	95.3	1	2
PDIA6	119	48.1	1	5
ACTN1	116	103	1	1
SPTAN1	107	284.4	1	1
DSTN	104	18.5	1	10
HPRT1	96	24.6	1	5
SERBP1	87	44.9	1	4
CRKL	87	33.8	1	4
SEC24C	80	118.2	1	2
COPB1	67	107.1	1	1
IPO5	66	123.6	1	2
CAD	63	242.8	1	1
CCT7	59.3	25	1	3
TMEM263	58	11.7	1	13
AHNAK	57	628.7	1	1
VCL	35	123.7	1	2
CSPG5	28	60	1	4
DYNC1H1	22	532.1	1	0
ATL2	0	66.2	1	3
OVOS2	0	161.1	1	2
P4HB	-	57.1	1	6
CLEC10A	-	35.4	1	4
KRT31	316	47.2	1	6
KRT9	83	62	2	3
PDHA1	36	43.3	1	3

Figure 3. 7 Mass Spectrometry Results. A. Venn diagram showing the numbers of proteins found in each list. For negative control, sample without H_2O_2 treatment was used. **B.** The first 15 candidate protein list. Only the 15 proteins found in replicate 1 and replicate 2 but not in negative control was used in this list. **C.** List of proteins found in only one replicate.

3.7. Enrichment Analysis

We performed gene ontology analysis using PANTHER and g:Profiler analysis tools with the proteins found in either one of the replicates **(Figure 3.8)**. We wanted to check what kinds of proteins were found in the proximity of STK10 and what were their functions. Most proteins found in this list were cytoskeletal proteins in both of the analyses. In our PANTHER analysis results, after cytoskeletal proteins, metabolite interconversion enzymes and protein modifying enzymes were found in the list **(Figure 3.8A)**.

A

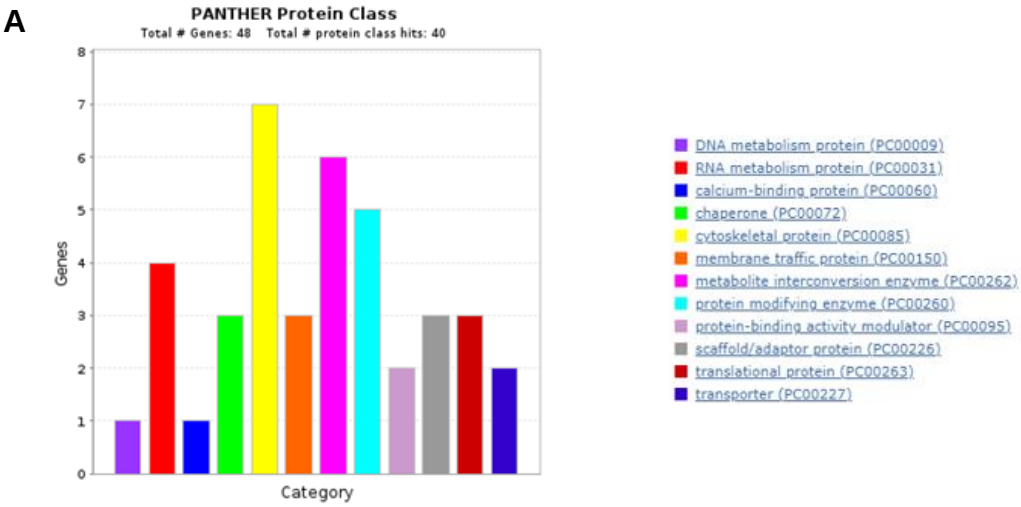

B

Figure 3. 8 Enrichment Analysis Results. A. Online PANTHER database was used for this analysis. Analysis was performed with the proteins found in either one of the replicate. **B.** Online g:Profiler tool was used for this enrichment analysis. g:GOSt functional profiling was done. Analysis was performed with the proteins found in either one of the replicates. Only the cytoskeleton-associated proteins were selected in this picture.

In our g:Profiler analysis, we again saw a similar picture where most of the proteins found in our list were cytoskeleton-associated proteins **(Figure 3.8B)**. Knowing that STK10 was associated with cell motility by its phosphorylation activity on ERM proteins, this result was expected and promising. These results may indicate that STK10 is affecting the breast cancer cells in a cytoskeleton-associated way. We continued with our analysis in this context.

3.8. Functions of The Proteins Found in The Proximity of STK10

We performed Reactome analysis with the proteins found in either one of the replicates and checked the most significant pathways found in the list **(Figure 3.9A)**. By doing so, we wanted to analyze the functions of the proteins found in our list.

A

Pathway name	Entities found	Entities Total	Entities ratio	Entities pValue
Regulation of RAS by GAPs	2	71	0.005	2.67E-2
Signaling by Non-Receptor Tyrosine Kinases	2	71	0.005	2.67E-2
Signaling by PTK6	2	71	0.005	2.67E-2
Oxygen-dependent proline hydroxylation of Hypoxia-inducible Factor Alpha	2	72	0.005	2.74E-2
G1/S DNA Damage Checkpoints	2	72	0.005	2.74E-2
Activation of NF-kappaB in B cells	2	72	0.005	2.74E-2
Cellular responses to stimuli	8	1,025	0.068	2.78E-2
Cdc20:Phospho-APC/C mediated degradation of Cyclin A	2	73	0.005	2.81E-2
Orc1 removal from chromatin	2	73	0.005	2.81E-2
HDR through Homologous Recombination (HRR)	2	73	0.005	2.81E-2
Signaling by Retinoic Acid	2	73	0.005	2.81E-2
Glyoxylate metabolism and glycine degradation	2	73	0.005	2.81E-2
Regulation of cytoskeletal remodeling and cell spreading by IPP complex components	1	8	0.001	2.81E-2
RHO GTPase Effectors	4	325	0.021	2.85E-2
Transcriptional Regulation by TP53	5	484	0.032	2.87E-2
AURKA Activation by TPX2	2	74	0.005	2.88E-2
APC/C:Cdh1 mediated degradation of Cdc20 and other APC/C:Cdh1 targeted proteins in late mitosis/early G1	2	74	0.005	2.88E-2
APC:Cdc20 mediated degradation of cell cycle proteins prior to satisfation of the cell cycle checkpoint	2	74	0.005	2.88E-2
Regulation of PTEN stability and activity	2	74	0.005	2.88E-2
CDK-mediated phosphorylation and removal of Cdc6	2	75	0.005	2.95E-2

Figure 3. 9 Functions of The Proteins Found in The Proximity of STK10.

Reactome analysis after running the proteins found in either one of the replicates in the Reactome Analysis Tool. p Value of all of them are <0.05.

From this analysis, we got some exciting results supporting the role of STK10 on cytoskeletal rearrangement. We found a protein has a role in cytoskeletal remodeling and cell spreading. Also, some of the proteins found close to STK10 had roles in regulating RAS, and RHO GTPase effectors. It is known that by activating a wide variety of downstream effectors that control cytoskeletal organization, intracellular trafficking, and transcription, RHO GTPases control cell behavior[34]. Since in some protein databases, STK10 has been associated with RAS superfamily proteins like KRAS, RhoA, and RhoB[35]**,** this finding of STK10's interaction partners having roles

in RAS protein regulation was promising. All these findings supported our hypothesis that STK10 affects cancer cells through cytoskeletal rearrangement.

3.9. STRING Analysis of the Proteins Found in the Proximity of STK10

We continued our experiments by performing STRING analyses using the first 15 protein list and the known interaction partners of STK10 **(Figure 3.10A)**. These analyses provided us with some encouraging findings. The fact that none of the proteins in our list was a known interaction partner of STK10 found in STRING database. This indicated the possible interaction partner we will find from our list will be a novel one.

When we ran the STRING analysis with medium confidence, we saw that two proteins in our list TAGLN2 (Transgelin 2) and TYK2 (Tyrosine Kinase 2) were found to be interacting with STK10's most known interaction partners Ezrin and Moesin proteins. Both of these proteins were associated with breast cancer before. TYK2 is a tyrosine kinase member of JAK family of kinases. It has been mostly related to cytokine-mediated inflammatory signaling, but recently, it has been identified as an oncogene driving cancer development and metastases [36]. TAGLN2 is an actin binding protein that has been associated with PI3K-AKT pathway and cancer invasion before. It has also been known to facilitate cytoskeletal structure formation in the cells [37]. Also, although it was not on our list, we wanted to check STK10's possible interaction with TAGLN. Mass spectrometry results are sometimes biased, and it may not give the full interactome of the protein of interest. We had a group working on TAGLN, which shows 65% similarity to TAGLN2, in our department in the context of breast cancer **(Figure S.1.1.)**. TAGLN is an actin-binding protein associated with breast cancer

epithelial to mesenchymal transition[38]. Because of this, we also wanted to check TAGLN-STK10 interaction.

A

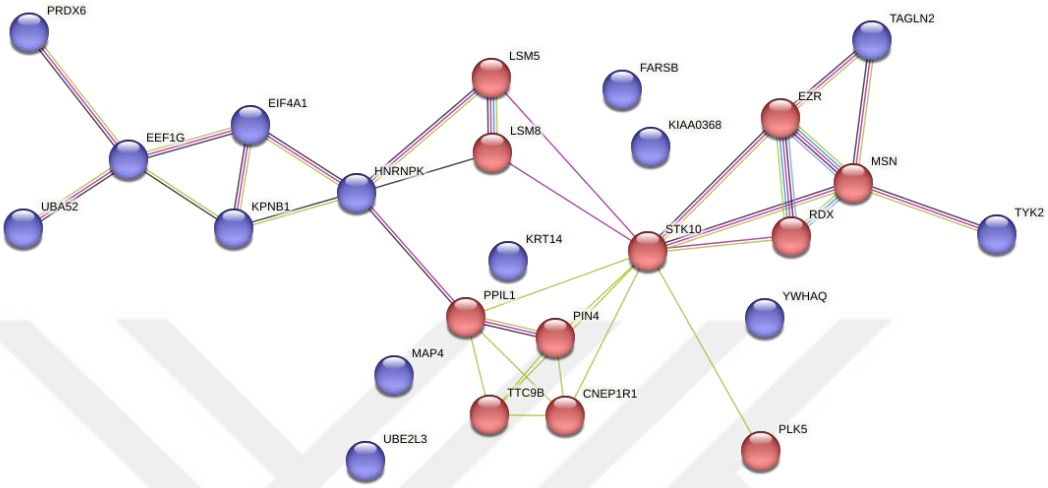

B

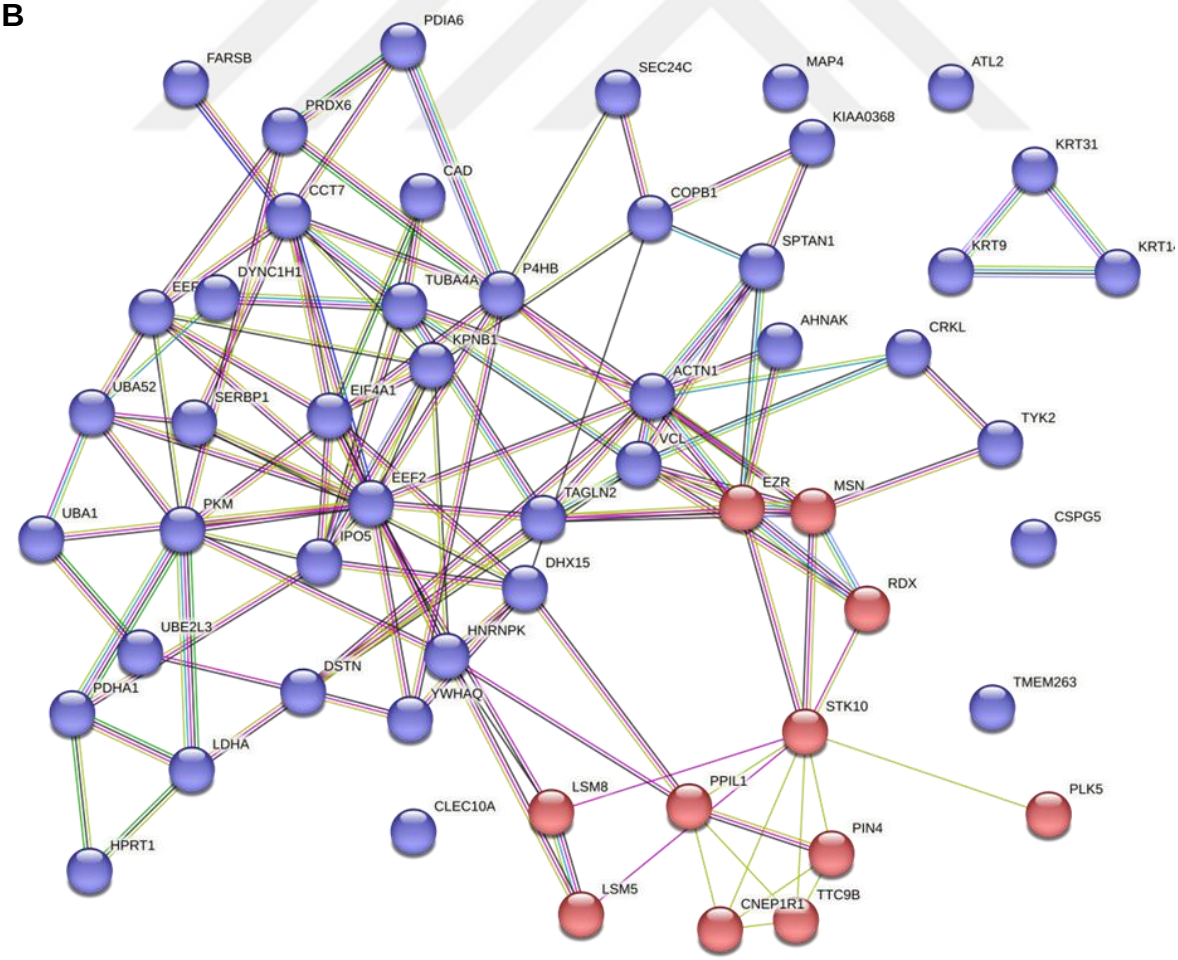

Figure 3. 10 STRING Analysis of the Proteins Found in the Proximity of STK10. STRING analysis results. Red bubbles indicate the known interaction partners of STK10 found in STRING database. Blue bubbles are the proteins found in our lists. The lines indicate the interaction evidence. More lines mean more significant interaction. **A.** The proteins found in both of the replicates were analyzed. **B.** Proteins found in either one of the replicates were analyzed for more comprehensive analysis.

In addition to these proteins, we selected HNRNPK protein that is also interacting with the known interaction partners of STK10. In a study about PDGF's effect on actin cytoskeleton, a rapid increase in HNRNPK protein phosphorylation was observed following PDGF stimulation. A novel regulatory mechanism involving HNRNPK activation is identified in the same study by which PDGF induces a sustained suppression of actin stress fibers and focal adhesions in fibroblasts[39]. Also, in another study, HNRNPK was sequestered in cytoplasm by intermediate filament protein KRT19. This sequestering was increasing HNRNPK's metastasis promoting activity[40].

After selecting these proteins, we wanted to make a more comprehensive analysis using the list of proteins found in either one of the replicates **(Figure 3.10B)**. The STRING analysis using this list indicated some more possible interaction partners of STK10. For instance, ACTN1 was found to be interacting with EZR. It is a cytoskeletal protein, and we wanted to focus on STK10's possible role in the cytoskeletal arrangement of breast cancer. Because of this, we selected ACTN1 as a candidate protein. ACTN1 is one of the alpha-actinin protein family members. In a study, hippo signaling activity was upregulated after ACTN1 knockdown, while Rho GTPase

activities were downregulated. In this study, they hypothesized that ACTN1 acts as a tumor promoter in hepatocellular carcinoma cells[41]. Then we selected CRKL, an oncogene that is known for its role in the activation of the RAS signaling pathway and fibroblast transformation. Also, it has been related to p110β dependent PI3K signaling[42]. Furthermore, there are studies showing CRKL is required for the migration and invasion of different cancer types [43].In addition to these proteins, even though they were not found to be directly interacting with STK10's known partners, we added DSTN and MAP4 to our list since they were also cytoskeleton-associated proteins. DSTN gene's product is a member of the actin-binding proteins. The actin turnover rate is increased by this protein family. Actin depolymerizing protein is encoded by this gene; it cleaves F-actin filaments and binds to G-actin monomers. A study showed DSTN contributes to lung adenocarcinoma progression by promoting cell migration, invasion, and EMT[44]. MAP4 (Microtubule-associated protein 4) has an important role in microtubule stability and assembly. This protein was found to be overexpressed in lung adenocarcinoma cells and it was suggested to be promoting tumor progression and migration[45]. To summarize, we focused our analyses on TAGLN2, TYK2, HNRNPK, ACTN1, CRKL, DSTN, MAP4 and TAGLN. We continued our bioinformatics analyses and performed some biochemical experiments using these proteins.

3.10. Co-Expression of The Candidate Proteins with STK10

We wanted to assess the possible interaction between STK10 and our selected proteins. For this purpose, we performed co-expression analyses with STK10 and the eight candidate proteins we had. We chose TNBC subtype specifically since our previous experiments indicated STK10's activity towards PI3K drug resistance is mainly enhanced in TNBC cells[21]. Although we hypothesized the interaction of

STK10 and the candidate proteins would be at the protein level rather than the RNA level. We suggested that if the expression of STK10 and the candidate protein correlates, this may indicate a possible shared role between them.

We found that CRKL, DSTN, and HNRNPK negatively correlated with STK10 with Pearson correlation scores of -0.27, -0.24, and -0.28, respectively **(Figure 3.11C,E, and G)**. Other than these genes, five other candidate gene expressions were found to be positively correlated with STK10 gene expression. We saw the most significant co-expression of STK10 with MAP4, TYK2, TAGLN2(Pearson correlation scores: 0.46, 0.35, 0.24 respectively.) **(Figure 3.11A,B,F)**.

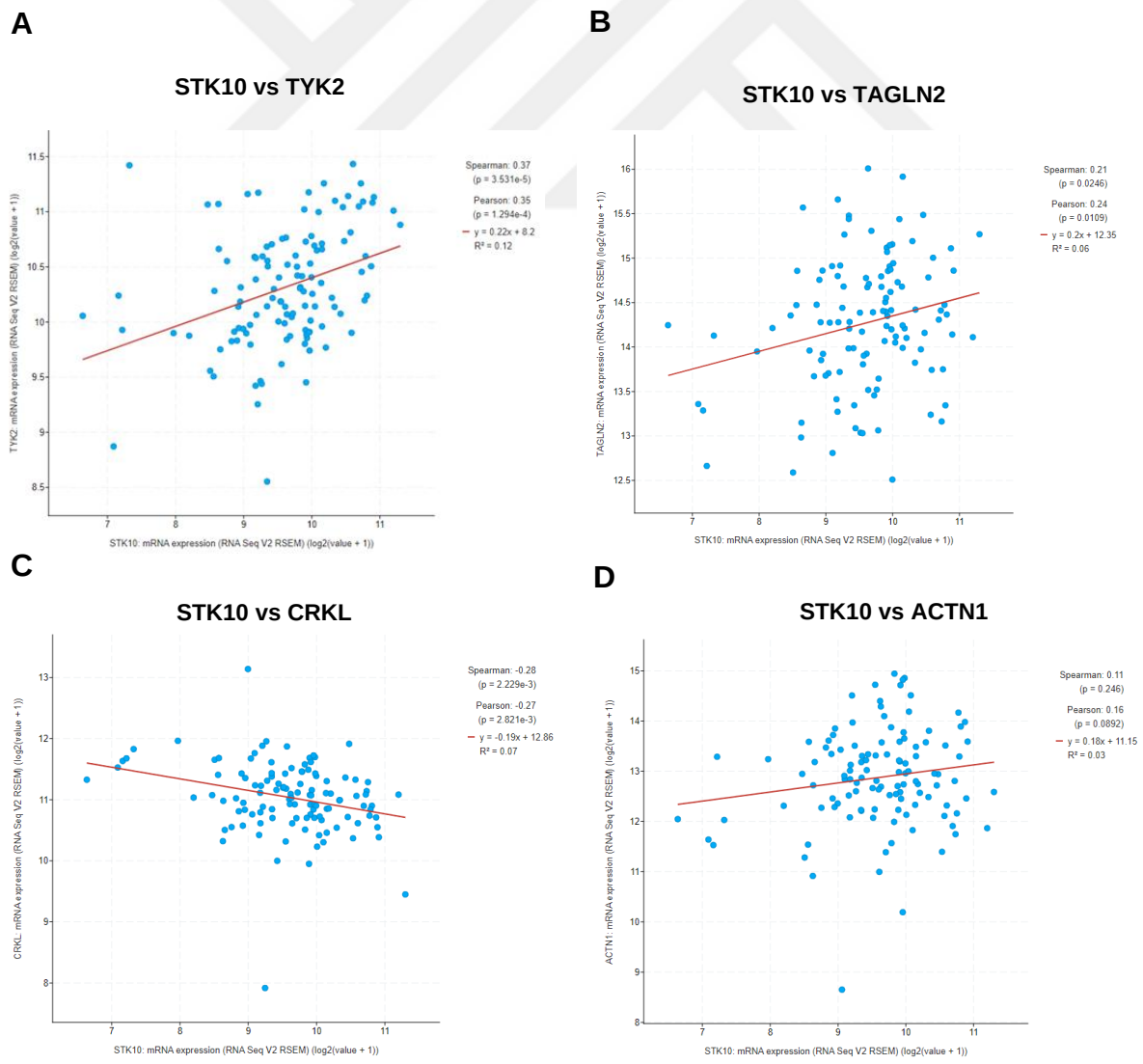

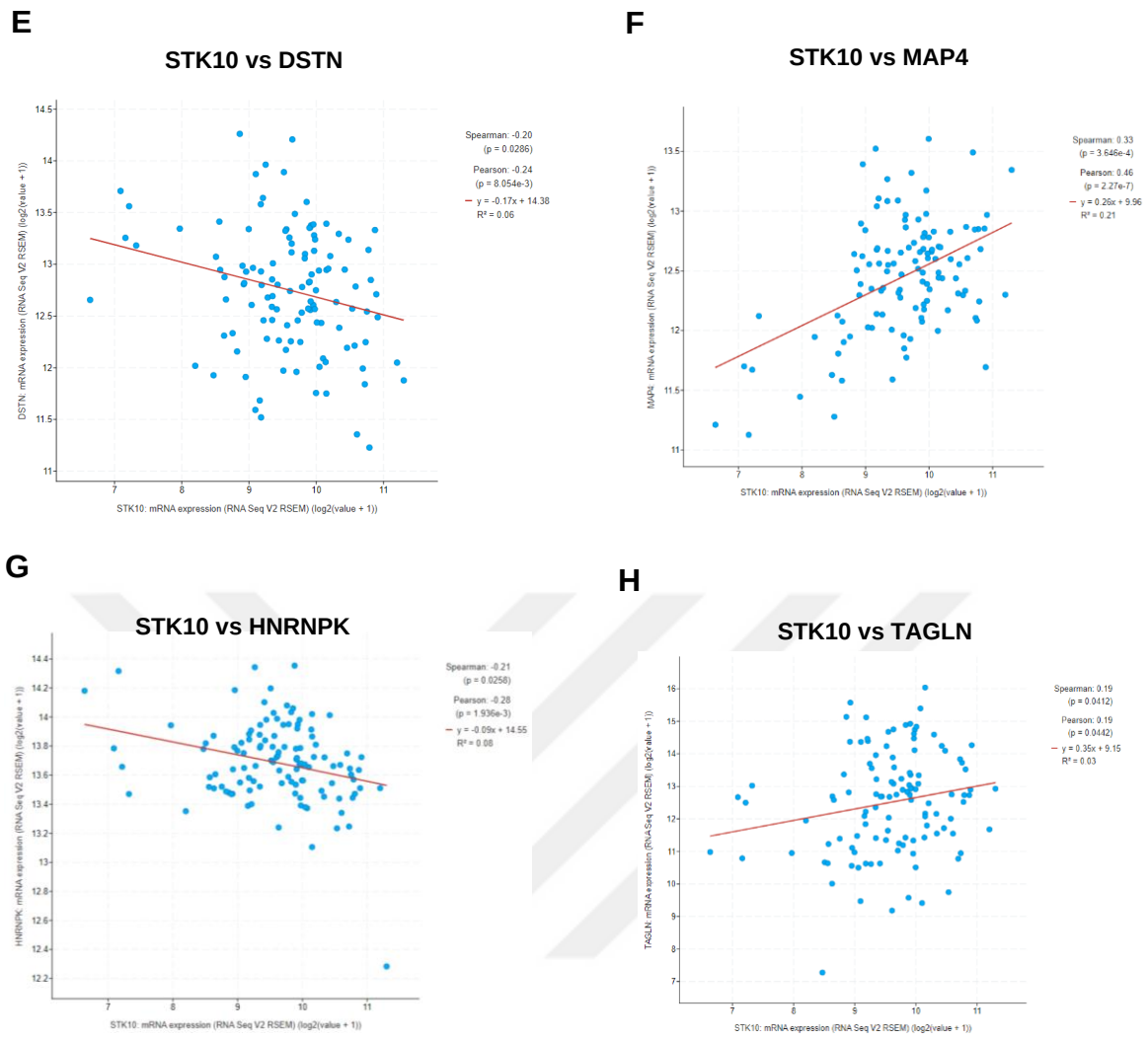

Figure 3. 11 Co-Expression of The Candidate Proteins with STK10. cBioPortal TCGA Firehose Legacy Breast Cancer database was used for the analysis. HER2, PR, ER negative subtype was selected manually. Co-expression analysis was done using RNA-Seq data. Graphs were drawn in log scale. **A.** STK10 mRNA expression vs. TYK2 mRNA expression. **B.** STK10 mRNA expression vs. TAGLN2 mRNA expression. **C.** STK10 mRNA expression vs. CRKL mRNA expression. **D. S**TK10 mRNA expression vs. ACTN1 mRNA expression. **E.** STK10 mRNA expression vs. DSTN mRNA expression. **F.** STK10 mRNA expression vs. MAP4 mRNA expression. **G.** STK10 mRNA expression vs. HNRNPK mRNA expression. **H.** STK10 mRNA expression vs. TAGLN mRNA expression.

DSTN is an actin depolymerization protein, and its expression is negatively correlated with STK10's expression in TNBC. Conversely, STK10 expression was positively correlated with actin-binding proteins ACTN1, TAGLN2, and TAGLN. This may indicate STK10 has a function in actin polymerization and regulation. TAGLN2 and TAGLN were linked to cancer cell proliferation and migration, highlighting their significance in this study. We also saw that STK10 expression correlates with microtubule-associated protein MAP4. In fact, this correlation had the highest correlation coefficient we saw in our results. In addition to the cytoskeletal proteins, we had proteins thought to be affecting cytoskeletal rearrangement in the cells, like HNRNPK and CRKL. STK10 had a negative correlation with HNRNPK in TNBC cells. So, they are probably not cooperating in the cells. They may have opposite functions. HNRNPK is localized to the cytoplasm with the help of keratin family proteins, and in the cytoplasm, it helps cancer metastasis[40]. Interestingly, our lists also had keratin family proteins like KRT9, KRT14, and KRT31. We can speculate STK10 has a role in the localization of HNRNPK in the cytoplasm.

STK10 also had a negative correlation with CRKL. CRKL is known to be promoting the proliferation and migration of cancer cells. Overexpression of CRKL causes actin cytoskeleton rearrangements[43]. All of these indicate STK10's possible role in cytoskeletal rearrangement by affecting actin, intermediate filament, and microtubule protein regulations in the cells. However, more research is required to understand how STK10 interacts with these proteins to produce these outcomes. In addition to the cytoskeletal proteins, a kinase, TYK2 was also positively correlated with STK10. TYK2, a Janus kinase (JAK) family member, mediates the signals of many cytokines involved in immune and inflammatory signaling. STK10 has also been associated with immune cell migration before. By phosphorylating ERM proteins, it causes immune

cell migration. So, the positive correlation between the expression of TYK2 and STK10 was not surprising to us. In addition to its role in the immune system, TYK2 was also found to be activated in cancer cells. Activation of TYK2 in cancer cells results in decreased cell death as well as increased cell growth and invasion[36]. STK10 and TYK2 may work together in both immune cells and cancer cells. They may promote migration in these cells.

3.11. Survival Analysis with the Candidate Proteins

To further analyze the interaction between STK10 and the candidate proteins, we performed survival analysis using online KmPlotter. We first plotted a survival plot of STK10 as a baseline. Then, we plotted survival plots for the candidate proteins. To check whether there is a correlation between STK10 and the candidate proteins, we plotted new graphs selecting the samples with high STK10 expression and checking the candidate proteins.

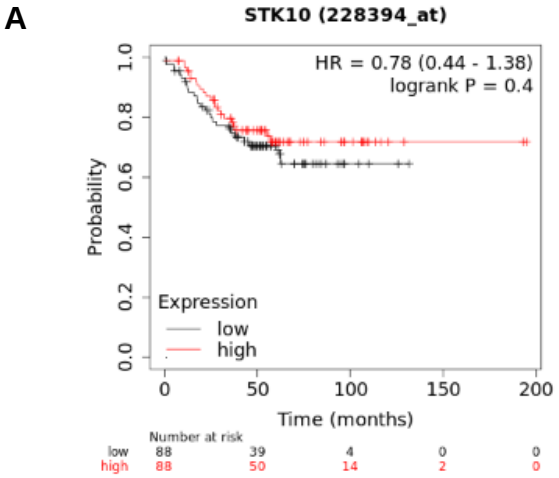

B

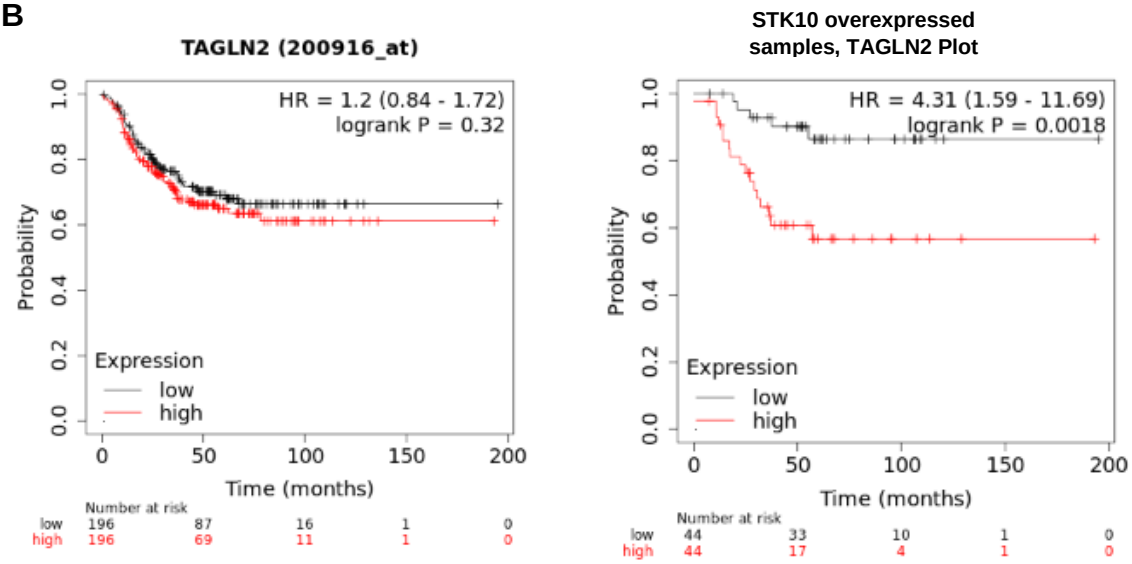
TAGLN2 (200916_at)
HR = 1.2 (0.84 - 1.72)
logrank P = 0.32
Probability
Expression
low
high
Time (months)
Number at risk
low 196 87 16 1 0
high 196 69 11 1 0
STK10 overexpressed samples, TAGLN2 Plot
HR = 4.31 (1.59 - 11.69)
logrank P = 0.0018
Probability
Expression
low
high
Time (months)
Number at risk
low 44 33 10 1 0
high 44 17 4 1 0

C

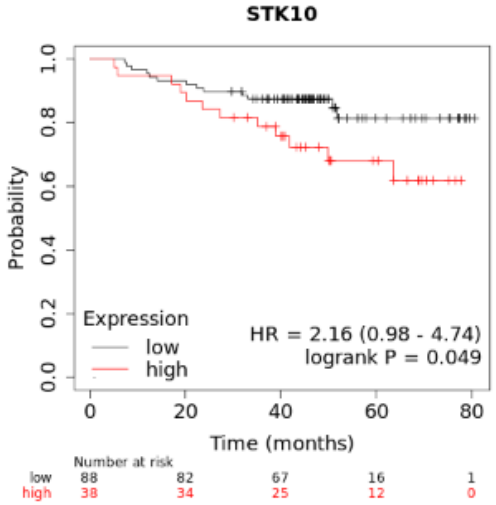
STK10
Probability
Expression
low
high
HR = 2.16 (0.98 - 4.74)
logrank P = 0.049
Time (months)
Number at risk
low 88 82 67 16 1
high 38 34 25 12 0

D

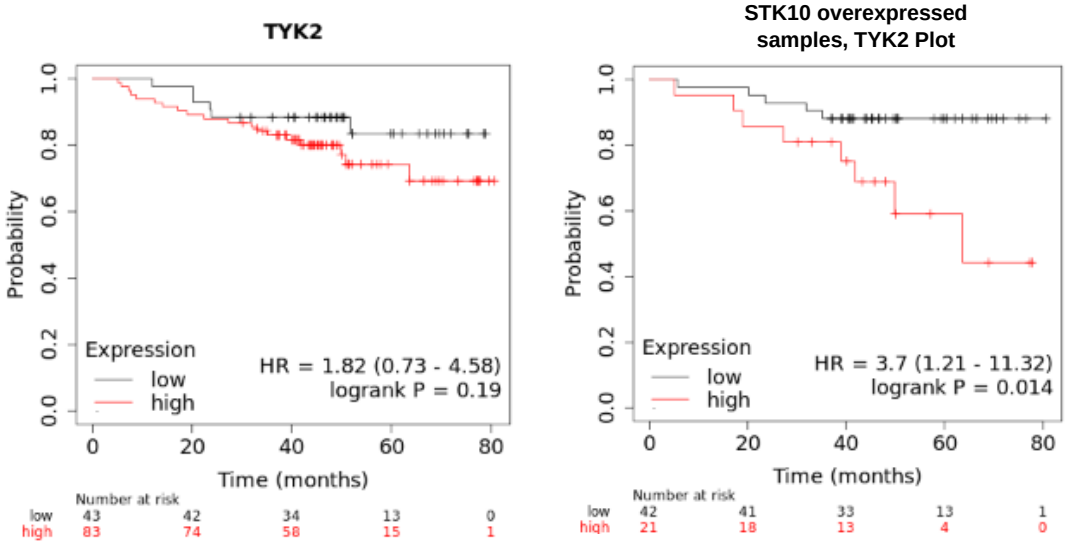
TYK2
Probability
Expression
low
high
HR = 1.82 (0.73 - 4.58)
logrank P = 0.19
Time (months)
Number at risk
low 43 42 34 13 0
high 83 74 58 15 1
STK10 overexpressed samples, TYK2 Plot
Probability
Expression
low
high
HR = 3.7 (1.21 - 11.32)
logrank P = 0.014
Time (months)
Number at risk
low 42 41 33 13 1
high 21 18 13 4 0

E

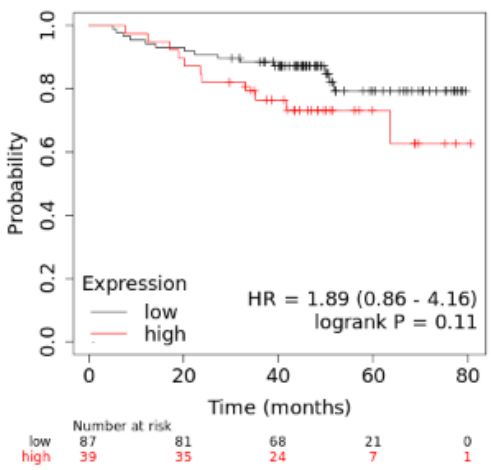

STK10 overexpressed samples, TAGLN Plot

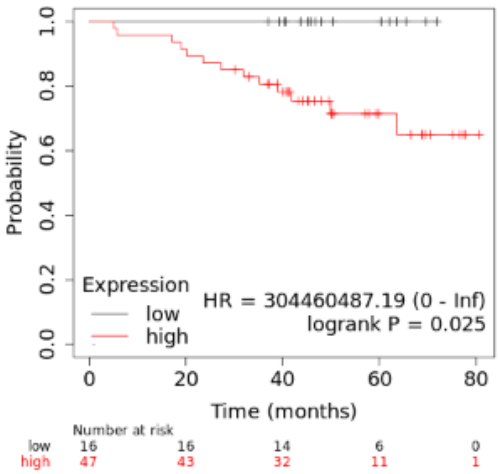

F

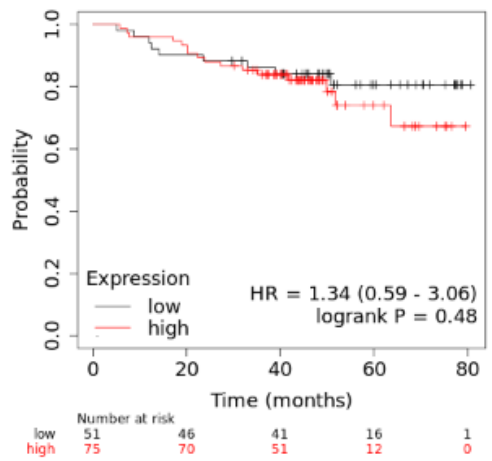

STK10 overexpressed samples, ACTN1 Plot

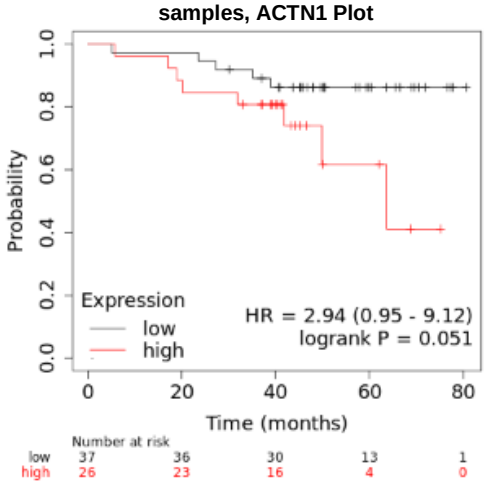

G

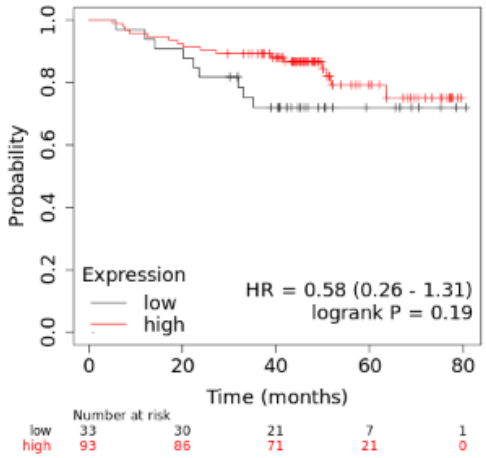

STK10 overexpressed samples, DSTN Plot

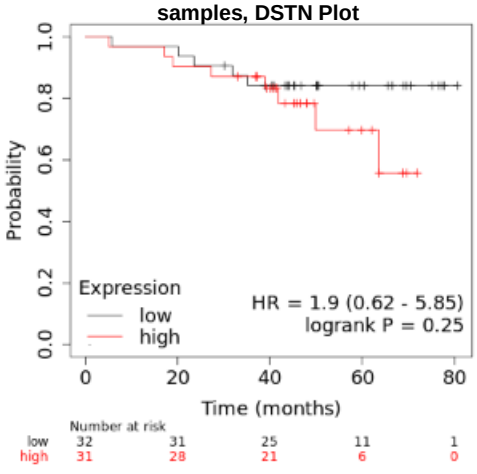

H

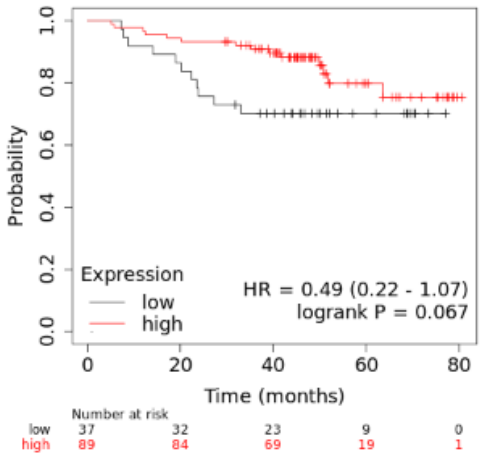

STK10 overexpressed samples, HNRNPK Plot

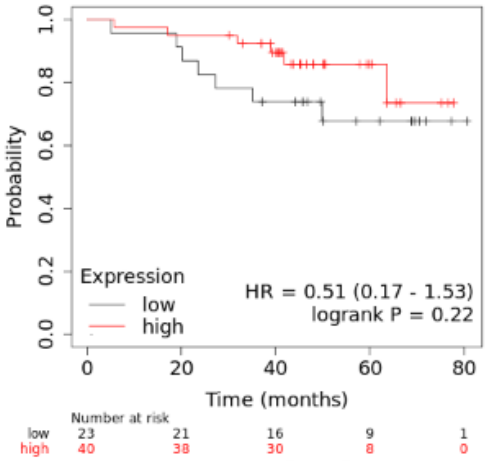

I

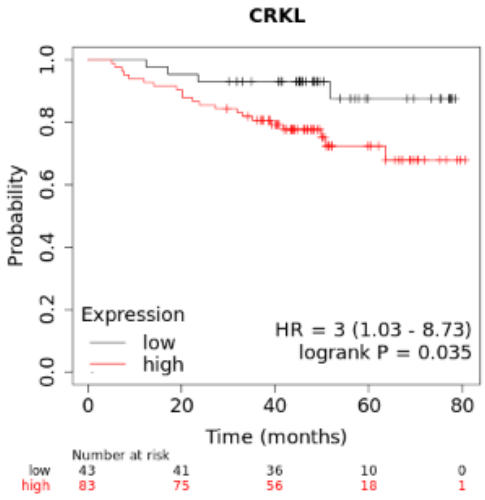

STK10 overexpressed samples, CRKL Plot

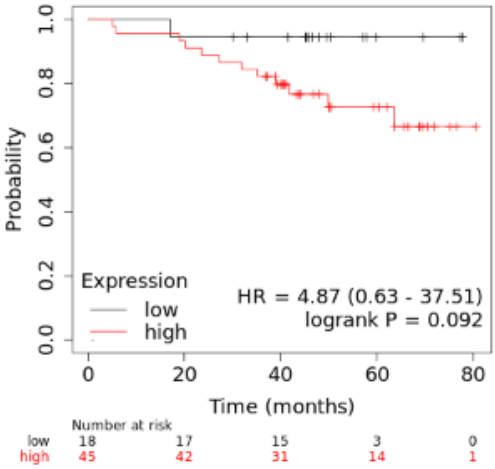

J

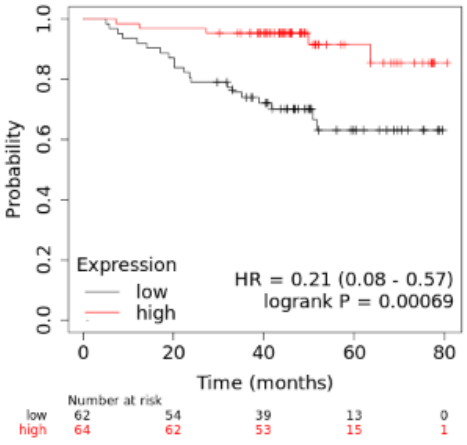

STK10 overexpressed samples, MAP4 Plot

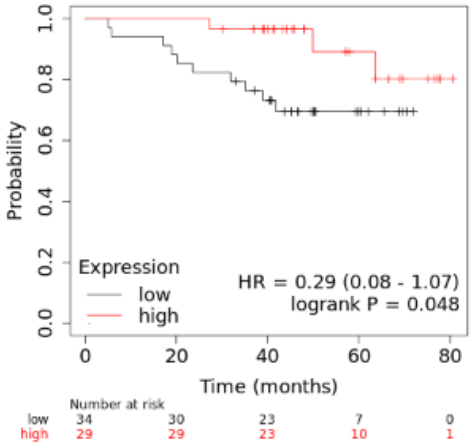

Figure 3. 12 Survival analysis with the candidate proteins. Online Kaplan Meier Plotter was used for the analysis. Manual selection for TNBC was done. For panels A-B, Gene-Chip database was used. For panel C-J, RNA-Seq database was used. On the left side, the survival analysis for the candidate proteins was performed. On the right side, the same analysis was performed by using only the STK10 overexpressed samples. **A.** STK10 Survival analysis using Gene-Chip data. **B.** TAGLN2 survival analysis using Gene-Chip data. **C.** STK10 survival analysis using RNA-Seq data. **D.** TYK2 **E.** TAGLN **F.** ACTN1 **G.** DSTN **H.** HNRNPK **I.** CRKL **J.** MAP4 survival analysis.

Overexpression of STK10 with four proteins (TAGLN2, TYK2, TAGLN, ACTN1) in our list resulted in a significant drop in the survival of the patients**(Figure 3.12A-F)**. These proteins were also found to have a positive correlation with STK10 in the co-expression analyses we performed **(Figure 3.11)**. This may suggest that STK10 works together with these proteins or maybe enhance their functions in cancer cells. These survival plots, when taken with the co-expression data, suggest a connection between STK10 and these four proteins. Since cancer is a heterogeneous disease, the proteins may act differently in different types of cancer subtypes, so the fact that we got these results from the specific subtype of breast cancer (TNBC) we are interested in is also very promising.

Overexpression of STK10 with other four proteins in the list (DSTN, HNRNPK, CRKL, and MAP4) did not result in a significant decrease in the survival of the patients**(Figure 3.12G-J)**. Overexpression of STK10 caused some decrease in patient survival when DSTN was overexpressed, though the effect was not significant. Patients whose DSTNs or HNRNPKs were overexpressed had a higher chance of survival, which

supports our hypothesis. In co-expression analyses **(Figure 3.11),** both of these proteins were found to be negatively correlated with STK10. We propose that STK10 promotes cancer cell malignancy, so the fact that these two proteins improve patients' chances of survival is promising for our hypothesis. As suggested before, it is possible that these proteins play antagonistic roles with STK10. Conversely, CRKL overexpression decreased the survival rate of the patients, and STK10 overexpression in these patients did not seem to be affecting the survival rate. However, given the negative correlation between STK10 and CRKL expression, the fact that STK10 overexpression did not reduce patient survival might make sense. It is possible that STK10 is negatively affecting CRKL's activity on cancer prognosis.

Unexpectedly, even though we observed a high positive correlation between STK10 and MAP4, the Km Plot analysis showed there was no impact of STK10 overexpression in MAP4 overexpressed patients. Furthermore, MAP4 overexpression increased the survival rate of the patients. Although this result is not supporting STK10-MAP4 interaction, more analyses are needed to be done in order to eliminate MAP4 as a candidate STK10 interactor.

3.12. Co-Localization of STK10 with TAGLN2

After our bioinformatics analyses, we wanted to verify the interactions biochemically. We performed immunofluorescence experiments to check the co-localization of STK10 with TAGLN2. We transfected HMEC-FLAG-APEX2-STK10 cells with eGFP-TAGLN2 vector and performed immunofluorescence experiment 48 hours after the transfection. We probed FLAG-STK10 with RFP. Our results **(Figure 3.13)** showed co-localization of STK10 with TAGLN2 in more than 60% of the cells having both GFP and RFP signal.

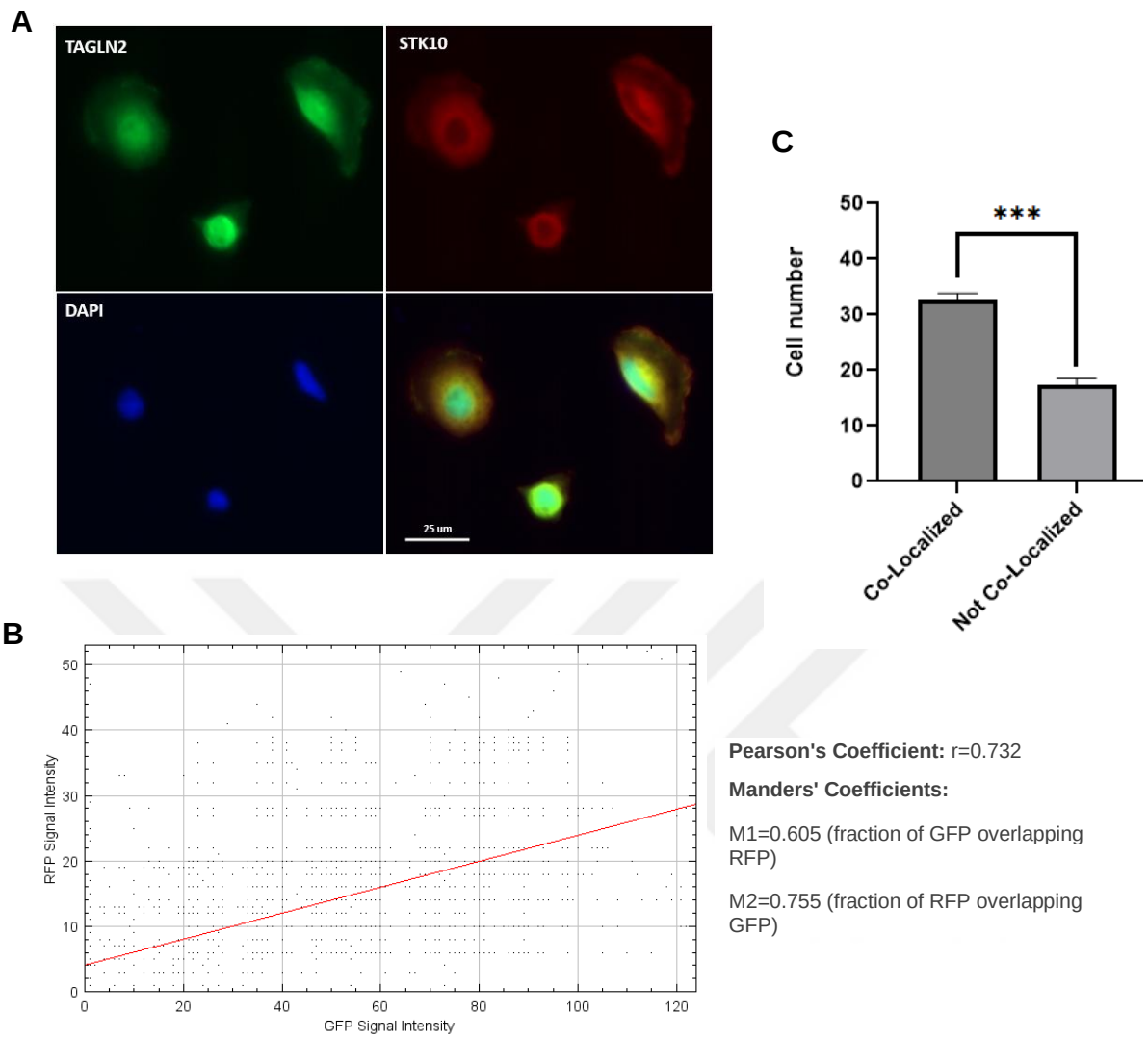

Figure 3. 13 Co-Localization of STK10 with TAGLN2. HMEC-Flag-APEX2-STK10 cells were seeded on cover slides and transfected with GFP-TAGLN2. After 48 hours of transfection, Flag proteins were tagged with RFP by performing immunofluorescence experiment. The cells were mounted with a mounting medium containing DAPI and the imaging was done using fluorescence microscopy. **A.** Immunofluorescence image, Green =TAGLN2, Red = STK10, Blue = DAPI. **B.** Quantification of panel B. Analysis of the image was done with ImageJ JACoP Plugin. Cytofluorogram was plotted for GFP-RFP signal intensities. (Pearson coefficient: r=0.732, Manders' Coefficients: M1: 0.605, M2=0.755.) **C.** Quantification of the immunofluorescence analysis. In 3 replicates, cells having GFP and RFP signals were

counted (150 cells in total). The ones showing colocalization were also counted and the bar graph was drawn. Using GraphPad Prism, Unpaired two tailed t-test was performed. (p value= 0.0008.)

We saw TAGLN2 signal coming from both the nucleus and perinuclear area. However, STK10 was depleted in the nucleus. It was mainly located in perinuclear and plasma membrane areas. To some extent, we saw colocalization of TAGLN2 and STK10 in the plasma membrane. But we saw the most significant colocalization of TAGLN2 and STK10 in the perinuclear area. Our quantifications also supported the co-localization of TAGLN2 and STK10 within the cells **(Figure 3.13.B-C)**. The fact that we saw both of these proteins localized in similar locations within the cells indicates TAGLN2 and STK10 working together. However, this interaction needs to be verified with further experiments in order to be certain. Confocal microscopic analyses may give us a better understanding of the localization of these two proteins.

3.13. Possible Interaction Between STK10- and TAGLN

As explained before, we also added TAGLN to our protein list since it has a similar protein structure to TAGLN2. For this purpose, we pulled down STK10 in HMEC-FLAG-APEX2 cells by performing FLAG-IP and performed western blotting with the eluate. We checked if TAGLN is coming with the precipitated STK10 or not.

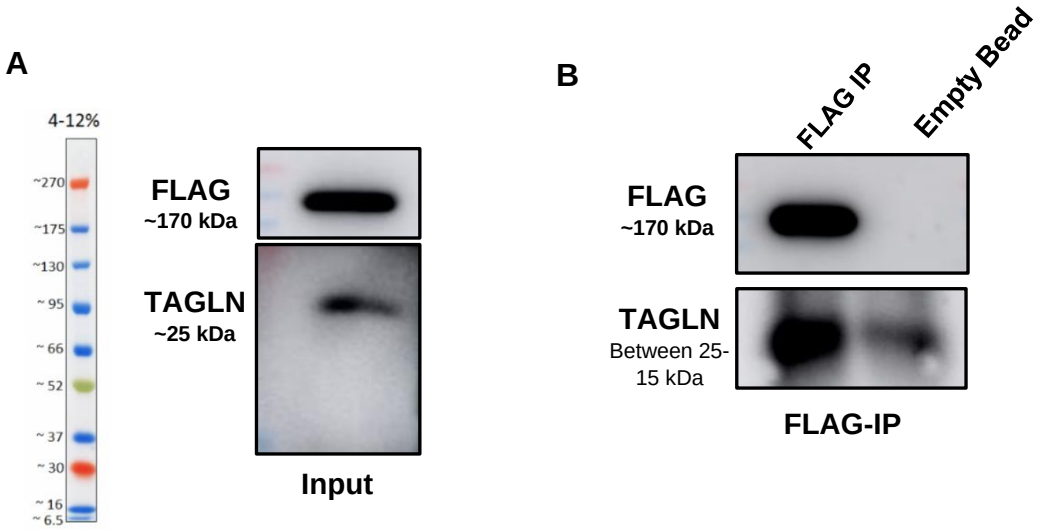

Figure 3. 14 Possible interaction between STK10- and TAGLN. Co-IP experiment was performed. FLAG tagged STK10 was pulled down with FLAG-IP, the sample was subjected to western blotting and probed with TAGLN primary antibody. **A.** Biolegend Protein Ladder and the input result using 40µg HMEC-Flag-APEX2-STK10 protein lysate. **B.** FLAG-IP result. 1mg protein lysate was used for each sample. As control, beads without FLAG antibody incubation were used.

We saw the TAGLN signal at 23 kda as expected in input. However, interestingly, in IP result, the TAGLN signal was coming from below 23 kDa. Sometimes, this can happen with immunoprecipitation products, it is an encountered phenomenon. Since the difference between the expected band and the observed bands was really small (Around 5-7 kDa) we assumed the bands we were seeing were the correct bands.

Unexpectedly, we also saw a similar signal in the negative control where we used empty beads. Although we saw this unexpected signal, the signal in FLAG-IP lane was much more prominent, and we suggest the signal we get from IP lane is showing TAGLN coming with STK10 pull-down. The TAGLN antibody we had may recognize a specific version of TAGLN protein. We have Myc-DDK tagged TAGLN containing plasmid in house, so we can transfect our cells with this plasmid and perform the pull-

down again. We can check the TAGLN signal with Myc specific antibody. By doing so, we can eliminate the possibility of TAGLN antibody recognizing a specific for of the protein. Although we need to repeat this experiment again with better controls, this result indicates a possible interaction between STK10 and TAGLN.

4. DISCUSSION

Breast cancer is the most common form of cancer in females worldwide. Also, it is the leading cause of death among female cancer patients globally. Breast cancer is a heterogeneous disease, so there are so many different ways to manage it. Women with early breast cancer without metastases undergo surgery. Most women also need systemic therapy. Systemic therapy can be given before surgery to reduce the tumor burden in women with large tumors. If surgical results or biomarkers suggest recurrence, adjuvant systemic therapy can be given. Many biomarkers are validated for systemic therapy decision-making. ER-positive and PR-positive breast cancer patients, regardless of HER2 status, should receive endocrine therapy to block ER activity[4]. There are more treatment options for hormone receptor-positive breast cancer types compared to hormone receptor-negative or triple-negative breast cancer (TNBC). The mainstay treatment for TNBC is chemotherapy, and there is a lack of routine targeted therapy for TNBC. It has short responses to chemotherapy and a poor overall survival rate[46]. Because of these, new therapy targets need to be find to treat TNBC efficiently.

The PI3-kinase (PI3K) signaling pathway has long been described, and it is well known that it plays an important role in breast cancer by linking receptor tyrosine kinase (RTK) signaling to the regulation of cell growth and survival. In patients with tumors harboring activating PIK3CA mutations, PI3Ka-specific inhibitors are showing promising results, though not all such tumors are sensitive to these inhibitors. In some other cases, despite early promising results, after treatment, inhibitor resistance is observed. Identifying patients more likely to respond to these inhibitors and developing therapeutic strategies to improve the clinical benefit requires an understanding of the

molecular mechanisms by which tumors bypass the pharmacological inactivation of PI3K. Studies trying to identify these mechanisms are focusing on AKT as the main protein relaying the signal to downstream targets. However, new studies illustrate some other mechanisms of PI3K inhibitor resistance, focusing on new targets (mainly kinases) working independently of AKT[19].

In order to find such a target, our group has done bioinformatical analyses using online tools and databases and selected STK10 as a candidate protein that would have a role in PI3K inhibitor resistance in breast cancer. Based on their bioinformatics analyses, they found that STK10 was highly upregulated in cells that were resistant to PI3K and AKT inhibitors. They also found that mRNA levels for STK10 were elevated in cells that were resistant to PI3K and AKT inhibition. STK10 was also a predictor of patient survival. When STK10 levels were high, survival was worse for all patients regardless of PIK3CA status, though the difference was most pronounced in PIK3CA mutant patients[21]. Hence, their biochemical results indicated STK10's possible interaction with PI3K pathway inhibitor resistance.

They also performed biochemical experiments to show STK10's impact on PI3K inhibitor resistance. They were able to sensitize PI3K inhibitor (BYL719) resistant MDA-MB-436 and BT20 cells to BYL-719 by knocking down STK10. They also showed that STK10 is overexpressed in another BYL-719-resistant cell line they had created, the T47D-BYLR cell line. However, they could not identify the molecular mechanism by which STK10 is affecting this inhibitor resistance. STK10 is not a very well-studied protein. Although there are some studies showing its possible interaction with cancer, its role in breast cancer is not known. In this study, we wanted to profile the interactome of STK10 in order to identify its interaction partners and have an understanding of its activity in breast cancer.

We used the technique of proximity-based biotinylation followed by mass spectrometry for this purpose. As the biotinylating enzyme, we used APEX2, which is an engineered peroxidase[23]. The selection of APEX2 was advantageous for our experimental procedure. In some of the other techniques utilized for protein-protein interaction analysis, such as affinity-based approaches followed by mass spectrometry, the transient interactions cannot be analyzed. The transiently or weakly interacting proteins of the protein of interest can be washed out during the washing steps. In proximity biotinylation, the tagging takes place in the live cell. Thanks to this, even the weak interactors of the protein of interest can be biotinylated. Also, this approach allows researchers to perform their experiments in a physiologically relevant environment. Compared to the other biotinylation enzymes, APEX2 is advantageous to use. For instance, the biotinylation with APEX2 can be activated by the addition of hydrogen peroxide to the environment of it, and the biotinylation can be done in minutes. In other techniques, biotinylation is generally done for hours. The fast-acting of APEX2 increases the specificity of the biotinylated proteins.

We used a two-step cloning strategy to produce the fusion protein encoding plasmid. Furthermore, we created an HMEC cell line stably expressing this fusion protein by performing retroviral transduction. We did not want to use cancer cells for our experiment because the protein-protein interactions in them are way more complex than normal cells. Inferring protein-protein interactions from cancer cells would be more problematic. So, we wanted to identify the partners of STK10 in a normal cell environment. HMEC cells we used were non-tumorigenic immortalized human mammary cells. Although these are normal cells, their physiology resembles TNBC. So, this cell line was an excellent choice for us to uncover the interactome of STK10 in breast cells in the context of TNBC.

We performed streptavidin pull-downs and did mass spectrometry analysis with the biotinylated proteins we pulled down. Our Gene Onthology and Reactome analyses using these proteins showed us that most of the proteins in our list were cytoskeleton-related proteins.

Previous studies of STK10, particularly its function in ERM phosphorylation, suggested the protein might be involved in cytoskeletal rearrangement and, consequently, cell migration. ERM proteins are linkers between the membrane and the cytoskeleton, and they play crucial roles in the control of cytoskeleton reorganization and subsequent alterations in cell morphology, migration, and adhesion. In their active form, ERM proteins connect the cytoskeleton to transmembrane proteins. As a result of its role in phosphorylating ERM proteins, STK10 has been linked to lymphocyte migration and adhesion. ERM proteins are also phosphorylated by Rho signaling with the help of Rho associated kinase (ROCK)[47].

STK10 has recently been linked to not only lymphocyte but also cancer cell migration. A group investigated the potential role of STK10 in tumor migration and invasion. In their first study, these researchers demonstrated that the absence of STK10 causes cervical cancer migration and invasion[16]. Also, the same group investigated the effect of STK10 KO on prostate cancer; their experiments suggested that STK10 may promote cell migration and prevent cell death in prostate cancer cells by inhibiting p38 MAPK [17]. Therefore, the fact that we observed an enrichment of cytoskeletal proteins in our results supports the notion that STK10 promotes cancer progression and migration via cytoskeletal rearrangement.

Cytoskeletal proteins, which include sub-families of proteins such as microtubules, actin, and intermediate filaments, are required for cell survival and cellular processes

in both normal and cancer cells. These mechanisms, however, can be altered in cancer cells to promote tumor development and progression, in which the functions of cytoskeletal proteins are co-opted to facilitate increased migratory and invasive capabilities, proliferation, and resistance to cellular and environmental stresses[48]. During tumorigenesis, the actin cytoskeleton becomes disorganized, which promotes tumor formation, survival, and metastasis by altering the nuclear:cytoplasmic ratio in cells. EMT is induced by reorganization of intermediate filaments in tumor cells; EMT promotes cell migration and invasion, leading to a more aggressive phenotype. Also, the resistance of tumor cells to chemotherapeutic drugs is associated with the differential expression of microtubule-associated proteins.

Ras super family member proteins like Rho are responsible for the changes in the actin cytoskeleton structure. In response to activation, Rho GTPases bind to a wide range of effectors, including protein kinases and some actin-binding proteins .These have an effect on local filamentous actin assembly or disassembly[49]. PI3K pathway can be activated via RAS protein. RAS also activates the Rho family GTPase Rac in a PI3K-dependent manner. Rac GTPase is a key mediator of oncogenic RAS transformation. Although the majority of published research suggests that Rac acts downstream of PI3K, several studies indicate that Rho GTPases can also activate PI3K. In addition, in some breast cancer studies, upregulation of PI3K signaling was found to be increasing invasion in a Rac-dependent but MAPK- and p70S6K-independent manner [50]. According to another study, the kinase activity of AKT is required to increase the levels of GTP-bound RhoA by phosphorylating DLC1[51]. PI3K pathway is also intertwined with RhoB protein. Normally, RhoB is repressed via the PI3K/Akt pathway. The upstream effects of RhoB on the PI3K/Akt pathway have been investigated in recent research. Ectopic expression of RhoB has been shown to

inhibit the PI3K/Akt pathway. However, under conditions of angiogenesis, RhoB can sustain Akt signaling. In a study, RhoB was shown to be inhibited by AKT signal, this inhibition in turn causes RhoB to feedback signal to AKT and upstream proteins in the pathway[52]. Additionally, activation of ROCK (Rho Associated Kinase) proteins induces direct phosphorylation of PTEN by ROCK, resulting in increased phosphatase activity of PTEN. Activated PTEN then directly opposes the survival-promoting PI3K/AKT pathway[53]. To summarize, the complex interaction between PI3K pathway-RAS family was suggested to lead to cytoskeletal rearrangement and differences in cell motility.

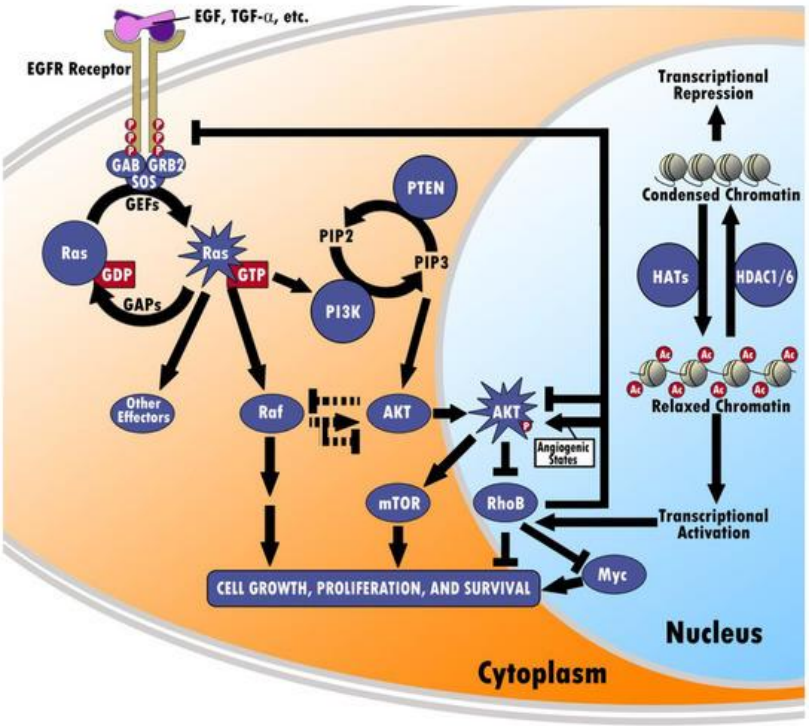

Figure 4. 1 RhoB affects PI3K Pathway with Feedback Signaling.
Schematic showing RhoB impact on PI3K pathway and AKT[52].

In some protein-protein interaction databases, STK10 is found to be interacting small GTPases, including KRAS, RHOA and RHOB[35]. Furthermore, our Reactome analysis indicated the interaction of STK10 with RHO GTPase and Ras signaling. From our Gene Onthology analyses, we saw an enrichment of cytoskeleton regulation

proteins in the interactome of STK10. Given that PI3K pathway is intertwined with Rho signaling **(Figure 4.1)** and Rho signaling can affect cytoskeletal remodeling, these results we got were promising.

All of the candidate proteins we selected were related to cytoskeletal remodelling except one: TYK2. TYK2 is a Janus Kinase family member. We selected this protein because it has been shown to interact with ERM proteins in immune-related cells. Since STK10 has also been shown to phosphorylate ERM proteins in the same context, we speculated that STK10 and TYK2 may interact. The fact that both of these proteins are kinases is also promising. However, the possible interaction between these proteins in breast cancer must be studied more to claim such things.

TAGLN and TAGLN2 were two of the cytoskeleton-related proteins we selected. They are from the transgelin family of proteins having actin-binding functions. Our wet lab experiments on these two proteins indicated their interaction with STK10. In various cancers, these proteins regulate migration, proliferation, and apoptosis[54]. Furthermore, both of these proteins were associated with breast cancer migration before[38], [55]. Interestingly, a study investigated TAGLN's activity on cytoskeletal rearrangement, and their results suggested that TAGLN affects cell motility through Rho GTPase pathway[56]. In another study, TAGLN was identified as a potent mechanosensitive gene capable of forming a regulation loop with Src activation in response to environmental stiffness, thereby mediating stiffness-regulated ovarian cancer progression by regulating the RhoA/ROCK pathway[57]. The interaction of TAGLN with ROCK (Rho associated kinase), a serine-threonine kinase, is exciting because ROCK proteins were known for their phosphorylation activity on ERM proteins, just like STK10[58]. Furthermore, ROCK has been related to PI3K pathway through PTEN activation. By looking at the literature and our results, we can speculate

the possible STK10 interaction with TAGLN has also connected to Rho proteins / Rho Kinases. RhoB activity can be affected by AKT,in turn, RhoB can negatively affect PI3K pathway and AKT by a feedback mechanism. STK10 and TAGLN may be involved in this interaction.

In addition to transgelin proteins, we identified other cytoskeleton-remodeling proteins in our list, including DSTN and ACTN1. DSTN is an actin-depolymerizing protein. It severs actin filaments (F-Actin). The actin turnover rate is increased in vivo thanks to this protein. Conversely, ACTN1 is an actin-bundling protein that crosslinks F-Actin to intracellular structures. Excitingly, in our co-expression analyses, we observed a positive correlation between STK10 and ACTN1 but a negative correlation between STK10 and DSTN. Our survival analyses were also supportive of these correlations. When STK10 and ACTN1 overexpression resulted in a significant drop in the survival of patients, STK10 and DSTN overexpression did not cause any significant difference in survival. Our results indicate STK10 positively affects ACTN1, whereas it negatively affects DSTN activity. Since these proteins work antagonistically, STK10's activation of only one of them makes sense. One might speculate STK10 impacts actin polymerization and depolymerization through these two proteins. However, more experiments are required before any such conclusions can be drawn.

Another candidate protein in our list was CRKL. It is an oncogene involved in the RAS signaling pathway's activation and fibroblast transformation. Also, it has been related to p110β dependent PI3K signaling previously[42]. As mentioned before, STK10 may act through RAS signaling pathway and help remodeling of the cytoskeleton. Although we did not observe a positive correlation between STK10 and CRKL, CRKL's interaction with PI3K pathway, RAS signaling, and cytoskeletal rearrangement makes

it an exciting candidate. We aim to uncover an interaction between STK10 and CRKL through our future experiments.

We also chose HNRNPK, which was found to be interacting with STK10's known partners in our STRING analysis. In a study, researchers showed PDGF suppresses actin stress fibers and focal adhesions in fibroblasts via a novel regulatory mechanism involving HNRNPK[39]. In another study, KRT19 sequestered HNRNPK in the cytoplasm, sequestering HNRNPK promoted metastasis [40]. Another protein we found to be correlating with STK10 was MAP4, a microtubule-associated protein. These findings show STK10's activity may affect not only actin proteins but also intermediate filaments and microtubules in the cells.

All these results indicated STK10's possible role in cytoskeletal rearrangement. Based on our results, it is possible that STK10 affects cytoskeletal proteins through a novel interaction with Rho signaling pathway. In this interaction, TAGLN, RhoB, RhoA, and ROCK may have roles. Especially TAGLN's association with ROCK and RhoA is indicative of this interaction.

5. CONCLUSION AND FUTURE PERSPECTIVES

To conclude, with our group's previous bioinformatics analyses, STK10 was selected as a candidate protein that may help the PI3K inhibitor resistance machinery in breast cancer cells AKT- independently.

The exact mechanism by which STK10 functions in cells and its interaction partners were not known before this study. So, in this project, we wanted to profile the interactome of STK10 and identify its novel interaction partners. With our proximity-based biotinylation experiments followed by mass spectrometry analysis, we were able to profile the proteins in close proximity to STK10. Our bioinformatics analyses using the proteins we identified after these experiments showed that most of them had roles in cytoskeleton remodeling and cell migration. Furthermore, some of them functioned in Rho signaling. STK10 and its known interaction partners have previously been associated with Rho proteins and Rho signaling. Likewise, PI3K pathway constituents have also been related to Rho proteins like RhoB.

With our immunofluorescence and Co-IP experiments, we were able to get promising results indicative of STK10 and transgelin family protein interaction, which are related to breast cancer migration. Moreover, TAGLN has also been associated with Rho signaling before. In light of these experiments, we can speculate that STK10 may have an activity on breast cancer cytoskeletal rearrangement, and it may do this by affecting TAGLN activity in the cells. This interaction may impact PI3K pathway and inhibitor resistance in breast cancer.

Although our results are promising, we need to do wet lab experiments to verify the interactions of our candidate proteins with STK10. We may perform Co-IP experiments

with more candidates and STK10. Furthermore, we can do other protein-protein interaction experiments like FRET (fluorescence resonance energy transfer) based assays. We can perform in vitro kinase assays to check if STK10 is phosphorylating the candidate proteins. Also, we can perform STK10 and candidate protein knock-downs or overexpressions. In these cells, we can check differences in Rho signaling pathway constituents, the migratory abilities of the cells, and their impact on PI3K pathway activity. Even though we performed our experiments in normal cells, these experiments can also be done on breast cancer cells instead of normal mammary cell lines. We can do more physiologically relevant profiling of the candidate proteins this way. At the end of these experiments, we hope to understand more about STK10 and its impact on PI3K inhibitor resistance of breast cancer.

6. BIBLIOGRAPHY

[1] "Cancer today," *Global CAncer Observatory: Cancer Today*, 2020. http://gco.iarc.fr/today/home (accessed Mar. 15, 2023).

[2] H. Sung *et al.*, "Global Cancer Statistics 2020: GLOBOCAN Estimates of Incidence and Mortality Worldwide for 36 Cancers in 185 Countries," *CA. Cancer J. Clin.*, vol. 71, no. 3, pp. 209–249, 2021, doi: 10.3322/caac.21660.

[3] R. L. Siegel, K. D. Miller, N. S. Wagle, and A. Jemal, "Cancer statistics, 2023," *CA. Cancer J. Clin.*, vol. 73, no. 1, pp. 17–48, 2023, doi: 10.3322/caac.21763.

[4] N. Harbeck *et al.*, "Breast cancer," *Nat. Rev. Dis. Primer*, vol. 5, no. 1, Art. no. 1, Sep. 2019, doi: 10.1038/s41572-019-0111-2.

[5] C. M. Perou *et al.*, "Molecular portraits of human breast tumours," *Nature*, vol. 406, no. 6797, Art. no. 6797, Aug. 2000, doi: 10.1038/35021093.

[6] L. Yin, J.-J. Duan, X.-W. Bian, and S. Yu, “Triple-negative breast cancer molecular subtyping and treatment progress,” *Breast Cancer Res.*, vol. 22, no. 1, p. 61, Jun. 2020, doi: 10.1186/s13058-020-01296-5.

[7] D. A. Fruman, H. Chiu, B. D. Hopkins, S. Bagrodia, L. C. Cantley, and R. T. Abraham, “The PI3K Pathway in Human Disease,” *Cell*, vol. 170, no. 4, pp. 605–635, Aug. 2017, doi: 10.1016/j.cell.2017.07.029.

[8] P. Singh, M. S. Dar, and M. J. Dar, “p110α and p110β isoforms of PI3K signaling: are they two sides of the same coin?,” *FEBS Lett.*, vol. 590, no. 18, pp. 3071–3082, 2016, doi: 10.1002/1873-3468.12377.

[9] Reprinted from “PI3K Pathway in Cancer.” by Biorender.com. Retrieved from https://app.biorender.com/illustrations/637dd791c9e4cb9d5fc7849f (accessed Apr. 30, 2023).

[10] J. J. Lee, K. Loh, and Y.-S. Yap, “PI3K/Akt/mTOR inhibitors in breast cancer,” *Cancer Biol. Med.*, vol. 12, no. 4, pp. 342–354, Dec. 2015, doi: 10.7497/j.issn.2095-3941.2015.0089.

[11] “STK10 serine/threonine kinase 10 [Homo sapiens (human)] - Gene - NCBI.” https://www.ncbi.nlm.nih.gov/gene/6793 (accessed Mar. 03, 2023).

[12] R. G. Fehon, A. I. McClatchey, and A. Bretscher, “Organizing the cell cortex: the role of ERM proteins,” *Nat. Rev. Mol. Cell Biol.*, vol. 11, no. 4, Art. no. 4, Apr. 2010, doi: 10.1038/nrm2866.

[13] L. Tao *et al.*, “Opposing roles of serine/threonine kinases MEKK1 and LOK in regulating the CD28 responsive element in T-cells,” *Biochem. J.*, vol. 363, no. Pt 1, pp. 175–182, Apr. 2002, doi: 10.1042/0264-6021:3630175.

[14] K. Fukumura *et al.*, “STK10 missense mutations associated with anti-apoptotic function,” *Oncol. Rep.*, vol. 30, no. 4, pp. 1542–1548, Oct. 2013, doi: 10.3892/or.2013.2605.

[15] S. Arora *et al.*, “RNAi phenotype profiling of kinases identifies potential therapeutic targets in Ewing’s sarcoma,” *Mol. Cancer*, vol. 9, no. 1, p. 218, Aug. 2010, doi: 10.1186/1476-4598-9-218.

[16] L. Zhang *et al.*, “Knockout of STK10 promotes the migration and invasion of cervical cancer cells,” *Transl. Cancer Res.*, vol. 9, no. 11, pp. 7079–7090, Nov. 2020, doi: 10.21037/tcr-20-1601.

[17] L. Zhang *et al.*, “STK10 knockout inhibits cell migration and promotes cell proliferation via modulating the activity of ERM and p38 MAPK in prostate cancer cells,” *Exp. Ther. Med.*, vol. 22, no. 2, p. 851, Aug. 2021, doi: 10.3892/etm.2021.10283.

[18] “Expression of STK10 in cancer - Summary - The Human Protein Atlas.” https://www.proteinatlas.org/ENSG00000072786-STK10/pathology (accessed Jan. 17, 2023).

[19] P. Castel *et al.*, “PDK1-SGK1 Signaling Sustains AKT-Independent mTORC1 Activation and Confers Resistance to PI3Kα Inhibition,” *Cancer Cell*, vol. 30, no. 2, pp. 229–242, Aug. 2016, doi: 10.1016/j.ccell.2016.06.004.

[20] A. Orlacchio *et al.*, “SGK1 Is a Critical Component of an AKT-Independent Pathway Essential for PI3K-Mediated Tumor Development and Maintenance,” *Cancer Res.*, vol. 77, no. 24, pp. 6914–6926, Dec. 2017, doi: 10.1158/0008-5472.CAN-17-2105.

[21] İ. O. Tarman, “Investigation of resistance mechanisms in response to PIK3CA inhibition in breast cancer,” Bilkent University, Ankara, 2020. [Online]. Available: http://repository.bilkent.edu.tr/handle/11693/54857

[22] W. Qin, K. F. Cho, P. E. Cavanagh, and A. Y. Ting, “Deciphering molecular interactions by proximity labeling,” *Nat. Methods*, vol. 18, no. 2, Art. no. 2, Feb. 2021, doi: 10.1038/s41592-020-01010-5.

[23] V. Hung *et al.*, “Spatially resolved proteomic mapping in living cells with the engineered peroxidase APEX2,” *Nat. Protoc.*, vol. 11, no. 3, Art. no. 3, Mar. 2016, doi: 10.1038/nprot.2016.018.

[24] J. A. Bosch and C. Chiao, “Proximity-dependent labeling methods for proteomic profiling in living cells: An update,” *WIREs Dev. Biol.*, vol. 10, no. 1, doi: 10.1002/wdev.392.

[25] R. E. Kingston, C. A. Chen, and H. Okayama, “Calcium Phosphate Transfection,” *Curr. Protoc. Cell Biol.*, vol. 19, no. 1, p. 20.3.1-20.3.8, 2003, doi: 10.1002/0471143030.cb2003s19.

[26] B. Tan, S. Peng, S. M. J. M. Yatim, J. Gunaratne, W. Hunziker, and A. Ludwig, “An Optimized Protocol for Proximity Biotinylation in Confluent Epithelial Cell Cultures Using the Peroxidase APEX2,” *STAR Protoc.*, vol. 1, no. 2, p. 100074, Jul. 2020, doi: 10.1016/j.xpro.2020.100074.

[27] D. Szklarczyk *et al.*, “The STRING database in 2023: protein-protein association networks and functional enrichment analyses for any sequenced genome of interest,” *Nucleic Acids Res.*, vol. 51, no. D1, pp. D638–D646, Jan. 2023, doi: 10.1093/nar/gkac1000.

[28] E. Cerami *et al.*, “The cBio cancer genomics portal: an open platform for exploring multidimensional cancer genomics data,” *Cancer Discov.*, vol. 2, no. 5, pp. 401–404, May 2012, doi: 10.1158/2159-8290.CD-12-0095.

[29] J. Gao *et al.*, “Integrative analysis of complex cancer genomics and clinical profiles using the cBioPortal,” *Sci. Signal.*, vol. 6, no. 269, p. pl1, Apr. 2013, doi: 10.1126/scisignal.2004088.

[30] B. Győrffy, “Discovery and ranking of the most robust prognostic biomarkers in serous ovarian cancer,” *GeroScience*, Mar. 2023, doi: 10.1007/s11357-023-00742-4.

[31] P. D. Thomas, D. Ebert, A. Muruganujan, T. Mushayahama, L.-P. Albou, and H. Mi, “PANTHER: Making genome-scale phylogenetics accessible to all,” *Protein Sci.*, vol. 31, no. 1, pp. 8–22, 2022, doi: 10.1002/pro.4218.

[32] U. Raudvere *et al.*, “g:Profiler: a web server for functional enrichment analysis and conversions of gene lists (2019 update),” *Nucleic Acids Res.*, vol. 47, no. W1, pp. W191–W198, Jul. 2019, doi: 10.1093/nar/gkz369.

[33] M. Gillespie *et al.*, “The reactome pathway knowledgebase 2022,” *Nucleic Acids Res.*, vol. 50, no. D1, pp. D687–D692, Jan. 2022, doi: 10.1093/nar/gkab1028.

[34] E. Sahai and C. J. Marshall, “RHO–GTPases and cancer,” *Nat. Rev. Cancer*, vol. 2, no. 2, Art. no. 2, Feb. 2002, doi: 10.1038/nrc725.

[35] “HIPPIE.” http://cbdm-01.zdv.uni-mainz.de/~mschaefer/hippie/query.php?s=stk10 (accessed May 04, 2023).

[36] D. C. Borcherding, K. He, N. V. Amin, and A. C. Hirbe, “TYK2 in Cancer Metastases: Genomic and Proteomic Discovery,” *Cancers*, vol. 13, no. 16, Art. no. 16, Jan. 2021, doi: 10.3390/cancers13164171.

[37] L. Wang *et al.*, “TAGLN2 promotes papillary thyroid carcinoma invasion via the Rap1/PI3K/AKT axis,” *Endocr. Relat. Cancer*, vol. 30, no. 1, Jan. 2023, doi: 10.1530/ERC-21-0352.

[38] N. Değer, “Functional analysis of transgelin in breast cancer,” Bilkent University, Ankara, 2018. [Online]. Available: http://repository.bilkent.edu.tr/bitstream/handle/11693/47663/10194357.pdf?sequence=1&isAllowed=y

[39] K. Nagano *et al.*, “PDGF regulates the actin cytoskeleton through hnRNP-K-mediated activation of the ubiquitin E3-ligase MIR,” *EMBO J.*, vol. 25, no. 9, pp. 1871–1882, May 2006, doi: 10.1038/sj.emboj.7601059.

[40] A. Fallatah *et al.*, “HNRNPK is retained in the cytoplasm by Keratin 19 to stabilize target mRNAs.” bioRxiv, p. 2022.01.24.477557, Jan. 25, 2022. doi: 10.1101/2022.01.24.477557.

[41] Q. Chen, X.-W. Zhou, A.-J. Zhang, and K. He, “ACTN1 supports tumor growth by inhibiting Hippo signaling in hepatocellular carcinoma,” *J. Exp. Clin. Cancer Res.*, vol. 40, no. 1, p. 23, Jan. 2021, doi: 10.1186/s13046-020-01821-6.

[42] J. Zhang *et al.*, “CRKL mediates p110β-dependent PI3K signaling in PTEN-deficient cancer cells,” *Cell Rep.*, vol. 20, no. 3, pp. 549–557, Jul. 2017, doi: 10.1016/j.celrep.2017.06.054.

[43] T. Park, “Crk and CrkL as Therapeutic Targets for Cancer Treatment,” *Cells*, vol. 10, no. 4, p. 739, Mar. 2021, doi: 10.3390/cells10040739.

[44] H.-J. Zhang *et al.*, “Destrin Contributes to Lung Adenocarcinoma Progression by Activating Wnt/β-Catenin Signaling Pathway,” *Mol. Cancer Res.*, vol. 18, no. 12, pp. 1789–1802, Dec. 2020, doi: 10.1158/1541-7786.MCR-20-0187.

[45] X. Xia, C. He, A. Wu, J. Zhou, and J. Wu, “Microtubule-Associated Protein 4 Is a Prognostic Factor and Promotes Tumor Progression in Lung Adenocarcinoma,” *Dis. Markers*, vol. 2018, p. 8956072, Mar. 2018, doi: 10.1155/2018/8956072.

[46] J. Pascual and N. C. Turner, “Targeting the PI3-kinase pathway in triple-negative breast cancer,” *Ann. Oncol.*, vol. 30, no. 7, pp. 1051–1060, Jul. 2019, doi: 10.1093/annonc/mdz133.

[47] M. Hébert, S. Potin, M. Sebbagh, J. Bertoglio, J. Bréard, and J. Hamelin, “Rho-ROCK-Dependent Ezrin-Radixin-Moesin Phosphorylation Regulates Fas-Mediated Apoptosis in Jurkat Cells1,” *J. Immunol.*, vol. 181, no. 9, pp. 5963–5973, Nov. 2008, doi: 10.4049/jimmunol.181.9.5963.

[48] M. S. Ong *et al.*, “Cytoskeletal Proteins in Cancer and Intracellular Stress: A Therapeutic Perspective,” *Cancers*, vol. 12, no. 1, p. 238, Jan. 2020, doi: 10.3390/cancers12010238.

[49] S.-T. Sit and E. Manser, “Rho GTPases and their role in organizing the actin cytoskeleton,” *J. Cell Sci.*, vol. 124, no. 5, pp. 679–683, Mar. 2011, doi: 10.1242/jcs.064964.

[50] O. Soriano, M. Alcón-Pérez, M. Vicente-Manzanares, and E. Castellano, “The Crossroads between RAS and RHO Signaling Pathways in Cellular Transformation, Motility and Contraction,” *Genes*, vol. 12, no. 6, Art. no. 6, Jun. 2021, doi: 10.3390/genes12060819.

[51] B. K. Tripathi *et al.*, “Receptor tyrosine kinase activation of RhoA is mediated by AKT phosphorylation of DLC1,” *J. Cell Biol.*, vol. 216, no. 12, pp. 4255–4270, Nov. 2017, doi: 10.1083/jcb.201703105.

[52] E. Gutierrez *et al.*, “Regulation of RhoB Gene Expression during Tumorigenesis and Aging Process and Its Potential Applications in These Processes,” *Cancers*, vol. 11, no. 6, Art. no. 6, Jun. 2019, doi: 10.3390/cancers11060818.

[53] C. A. Street and B. A. Bryan, “Rho Kinase Proteins—Pleiotropic Modulators of Cell Survival and Apoptosis,” *ANTICANCER Res.*, 2011.

[54] J. Liu, Y. Zhang, Q. Li, and Y. Wang, “Transgelins: Cytoskeletal Associated Proteins Implicated in the Metastasis of Colorectal Cancer,” *Front. Cell Dev. Biol.*, vol. 8, 2020, Accessed: May 09, 2023. [Online]. Available: https://www.frontiersin.org/articles/10.3389/fcell.2020.573859

[55] L. Liu *et al.*, “Transgelin 2 Promotes Paclitaxel Resistance, Migration, and Invasion of Breast Cancer by Directly Interacting with PTEN and Activating PI3K/Akt/GSK-3β Pathway,” *Mol. Cancer Ther.*, vol. 18, no. 12, pp. 2457–2468, Dec. 2019, doi: 10.1158/1535-7163.MCT-19-0261.

[56] Z.-X. Lew *et al.*, “Transgelin interacts with PARP1 in human colon cancer cells,” *Cancer Cell Int.*, vol. 20, p. 366, 2020, doi: 10.1186/s12935-020-01461-y.

[57] X. Wei *et al.*, “TAGLN mediated stiffness-regulated ovarian cancer progression via RhoA/ROCK pathway,” *J. Exp. Clin. Cancer Res.*, vol. 40, no. 1, p. 292, Sep. 2021, doi: 10.1186/s13046-021-02091-6.

[58] M. A. Haas, J. C. Vickers, and T. C. Dickson, “Rho kinase activates ezrin-radixin-moesin (ERM) proteins and mediates their function in cortical neuron growth, morphology and motility in vitro,” *J. Neurosci. Res.*, vol. 85, no. 1, pp. 34–46, Jan. 2007, doi: 10.1002/jnr.21102.

[59] G. Housman *et al.*, “Drug Resistance in Cancer: An Overview,” *Cancers*, vol. 6, no. 3, pp. 1769–1792, Sep. 2014, doi: 10.3390/cancers6031769.

[60] P. Liu, H. Cheng, T. M. Roberts, and J. J. Zhao, “Targeting the phosphoinositide 3-kinase pathway in cancer,” *Nat. Rev. Drug Discov.*, vol. 8, no. 8, Art. no. 8, Aug. 2009, doi: 10.1038/nrd2926.

[61] P. Singh, M. S. Dar, and M. J. Dar, “p110α and p110β isoforms of PI3K signaling: are they two sides of the same coin?,” *FEBS Lett.*, vol. 590, no. 18, pp. 3071–3082, 2016, doi: 10.1002/1873-3468.12377.

[62] A. L. Neisch and R. G. Fehon, “Ezrin, Radixin and Moesin: Key regulators of membrane-cortex interactions and signaling,” *Curr. Opin. Cell Biol.*, vol. 23, no. 4, pp. 377–382, Aug. 2011, doi: 10.1016/j.ceb.2011.04.011.

[63] M. Arnold *et al.*, “Current and future burden of breast cancer: Global statistics for 2020 and 2040,” *The Breast*, vol. 66, pp. 15–23, Dec. 2022, doi: 10.1016/j.breast.2022.08.010.

[64] G. Alanis-Lobato, M. A. Andrade-Navarro, and M. H. Schaefer, “HIPPIE v2.0: enhancing meaningfulness and reliability of protein–protein interaction networks,” *Nucleic Acids Res.*, vol. 45, no. D1, pp. D408–D414, Jan. 2017, doi: 10.1093/nar/gkw985.

7. APPENDIX

7.1 Supplementary Figures

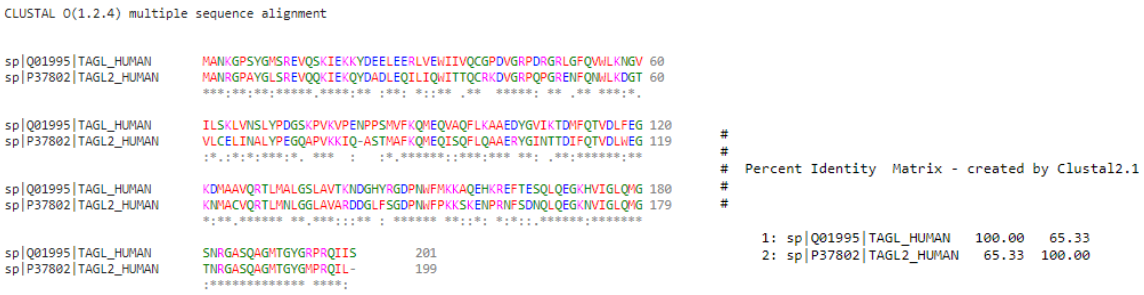

Figure S.1. 1 TAGLN -TAGLN2 Multiple Sequence Alignment. The multiple sequence alignment was performed using Clustal Omega. TALGN and TAGLN2 are 65% similar to each other.

interactor - UniProt id	interactor - Entrez gene id	interactor - gene symbol	score (click on a score value to see the evidence)
STK10_HUMAN	6793	STK10	0.87
RHOB_HUMAN	388	RHOB	0.82
LAMP1_HUMAN	3916	LAMP1	0.73
RASK_HUMAN	3845	KRAS	0.73
NONO_HUMAN	4841	NONO	0.72
ARF6_HUMAN	382	ARF6	0.63
CAV1_HUMAN	857	CAV1	0.63

Figure S.1. 2 HIPPIE analysis of STK10. The analysis shows the proteins interacting with STK10. The proteins with the highest evidence scores were selected.

7.2 Copyright Permission

Copyright for Figure 4.1:

“All MDPI journals are Open Access and subject to the Creative Commons Attribution License (CC BY). The CC BY permits unrestricted use, distribution, and reproduction